Available online at www.sciencedirect.com
ScienceDirect
Geochimica et Cosmochimica Acta 70 (2006) 5488–5506
Geochimica
www.elsevier.com/locate/gca

A method for activity calculations in saline and mixed solvent solutions at elevated temperature and pressure: A framework for geological phase equilibria calculations

Katy Evans [a,b,*], Roger Powell [b]

[a] CSIRO Exploration and Mining, School of Earth Sciences, University of Melbourne, Vic. 3010, Australia
[b] School of Earth Sciences, University of Melbourne, Vic. 3010, Australia

Received 4 October 2005; accepted in revised form 22 August 2006

Abstract

Quantitative thermodynamic calculations that involve aqueous fluids have proved difficult because of the complexity of the interactions that occur within the fluids. Existing thermodynamic models are difficult to apply to mixed solvent or highly saline solutions at $P > 0.3$ GPa and $T > 300$ °C. This work constructs a method for activity–composition calculations in saline, mixed solvent, supercritical aqueous solutions. Mixing is formulated on a mole-fraction scale in terms of a set of independent end-members that describe composition and speciation within the solution. The ideal mixing term takes speciation into account and avoids problems with the common ion effect. Non-ideal interactions are represented by an activity coefficient term that combines a limited form of Debye–Hückel and a van Laar formulation. This approach, referred to as the DH–ASF model, is thermodynamically valid over a wide range of P, T and fluid composition. The value of the model lies in its broad applicability, and small number of calibration parameters. Experimental data from the literature for the systems NaCl–H_2O, KCl–H_2O, H_2O–SiO_2–CO_2, H_2O–NaCl–CO_2, H_2O–NaCl–SiO_2 and for H_2O–albite melts have been used to calibrate the DH–ASF model. Calculations were performed using THERMOCALC, computer software that calculates equilibria for mineral-based chemical systems.[1] The model represents the data to within experimental error in most cases. Conditions modelled include pressures between 0.2 and 1.4 GPa, temperatures between 500 and 900 °C, and x_{H_2O} from 0.1 to 1. Calibrated parameters are consistent with expectations based on the conceptual model for the fluid, and are relatively insensitive to changes in pressure and temperature for most examples. The DH–ASF model is thermodynamically valid for a range of P–T conditions that includes pressures from 0.1 to 2 GPa and temperatures from 200 to 1000 °C. A lack of experimental data restricts calibration of the model for many end-members. However, it may be possible to neglect parameters associated with end-members present in small amount. In this case, or with new experimental data for calibrations, the DH–ASF model allows previously inaccessible geological systems and processes to be modelled.

1. Introduction

Aqueous solutions at high pressure and temperature affect the rocks that they interact with. Fluids play a critical role in the formation of ore deposits (e.g., Gibert et al., 1992; Cox, 1995), the composition of subducting material (e.g., Ayers and Watson, 1991), mantle metasomatism (e.g., Stalder et al., 1998), hydrothermal alteration of the ocean floor (e.g., Alt et al., 1998), and the evolution of vapour-saturated melts (e.g., Lowenstern, 2001). Thermodynamic calculations are used to predict and interpret the characteristics of these aqueous solutions. The effects of mixing between solutes and solvents significantly affect solution properties but such effects are difficult to integrate into thermodynamic models. The thermodynamic effects of mixing are described using activity–composition

* Corresponding author. Fax: +61 2 61250738.
E-mail address: Katy.evans@anu.edu.au (K. Evans).

[1] The current version of THERMOCALC and the internally consistent dataset can be obtained from http://www.earthsci.unimelb.edu.au/tpg/thermocalc/.

0016-7037/$ - see front matter © 2006 Elsevier Inc. All rights reserved.
doi:10.1016/j.gca.2006.08.032

relationships, which are commonly split into ideal and non-ideal contributions (e.g., Powell, 1977; Helgeson et al., 1981; Li et al., 1994).

The ideal mixing activity is linked to solute concentrations, and is commonly specified to be the mole fraction or molality of the solute of interest (e.g., Anderson and Crerar, 1993). However, speciation of solutes can result in incorrect representation of the ideal mixing by solute concentrations. (e.g., Stokes and Robinson, 1948; Pelton and Thompson, 1970). For example, dissociation of NaCl results in a doubling of the number of solute molecules, so that an ideal mixing term based on the number of moles of NaCl added to the solution will overestimate the ideal activity of this solute. A further complication in the formulation of the ideal activity is the common ion effect, which occurs when two or more salts that share a common ion (e.g., NaCl and KCl) are added to a solution. The concentration of the common ion is then a function of the concentration of both salts, and the ideal activity of either salt cannot be calculated solely from the number of moles of either salt in the solution. An additional factor is the choice of concentration scale. Many models use the molal concentration scale, but this is unsuitable for concentrated or mixed solvent solutions because molality becomes a non-linear function of concentration and then approaches infinity as the mole fraction of water decreases towards zero.

The most used expressions for the activity coefficient in geological applications are the Debye–Hückel limiting law (e.g., Bockris and Reddy, 1998), and extended versions of this formulation (e.g., Davies, 1962; Truesdell and Jones, 1974; Helgeson et al., 1981). These expressions represent the behaviour of solutes in aqueous solutions at ionic strengths of up to 0.1 molal very successfully. Their use is limited though, because geological solutions may reach ionic strengths of up to 15 molal. Activity coefficient expressions for aqueous solutions at higher ionic strength are provided by the work of Pitzer and co-workers (Pitzer, 1973; Pitzer and Simonson, 1986; Clegg and Pitzer, 1992; Clegg et al., 1992). The Pitzer formulations predict the properties of salt-bearing aqueous solutions accurately over the entire range of composition from dilute aqueous solutions to fused salt mixtures. However, they cannot be used to describe solutions at temperatures and pressures much different to those of the original calibration, or to calculate the properties of mixed-solvent solutions. Mixed solvent solutions are common in geological environments (e.g., Baker et al., 1991; Phillips and Powell, 1993; Ferry, 1994; Lowenstern, 2001), and can have different properties to aqueous solutions (e.g., Walther, 1992). The chemical engineering literature provides activity coefficient formulations that can be applied to mixed solvent electrolyte solutions (e.g., Cardoso and O'Connell, 1987; Li et al., 1994; Wang et al., 2002; Chen and Song, 2004: see review by Anderko et al., 2002). The majority of such models split the excess energy of mixing into long, medium and short range contributions. The contributions are typically represented by one or more of: a Debye–Hückel (Debye and Hückel, 1923) or Mean-Sphere Approximation (e.g., Blum and Hoye, 1977; Gering et al., 1989) term to represent long range interactions, a virial term dependent on temperature and ionic strength (e.g., Wang et al., 2002) for medium range interactions, and a short range interaction model such as NRTL (Renon and Prausnitz, 1968), UNIQUAC or UNIFAC (Abrams and Prausnitz, 1975), respectively. These models are generally unsuitable for geological applications because they either (a) neglect speciation and/or (b) use standard states and/or concentration scales unsuitable for solutions where $X(H_2O)$ is low and/or (c) require numerous calibration parameters that are unavailable at the pressures and temperatures of interest.

Our work involves a model that can account for ideal and non-ideal activity in mixed solvent, supercritical, high pressure ($P > 0.2$ Gpa) and high temperature ($T > 300$ °C) solutions over a wide range of concentrations. The approach uses a mole fraction concentration scale, and calculates ideal activity with expressions that take the configuration of the ions in solution into account. This approach allows common ion effects to be avoided. A limited Debye–Hückel term that can be applied to mixed solvents and concentrated solutions, is combined with a multi-component Van Laar formulation to calculate activity coefficients. Each of the parts of the model has been shown to be effective in other formulations or applications. The ideal mixing term is derived from the approach to mineral activity–composition relationships described in papers by Powell, Holland and coworkers (e.g., Powell, 1977; Holland and Powell, 1996a; Holland and Powell, 1996b), while Debye–Hückel and Van Laar terms have been used in previous activity coefficient formulations (e.g., Helgeson et al., 1981; Holland and Powell, 2003). The unique features of the model are the choice of the elements of the model, the wide range of solutions and P/T conditions that can be described using a small number of parameters, and in the capacity to use explicit conceptual models for speciation. The model is calibrated using experimental data for systems of interest over a range of pressures and temperatures, and the predictive powers of the model are discussed.

2. Terminology

A phase is defined as "a homogeneous body of matter, generally having distinct boundaries with adjacent phases, and, so in principle, being mechanically separable from them" (Anderson and Crerar, 1993). The chemical components of the system are the smallest set of chemical formulae required to describe the composition of all the phases in the system (c.f. Anderson and Crerar, 1993; Nordstrom and Munoz, 1994). The term species refers to an actual molecular or ionic entity which has existence as an identifiable unit (Anderson and Crerar, 1993; Nordstrom and Munoz, 1994). An end-member is a chemical entity of fixed composition that may be observable or hypothetical (e.g., Thompson, 1982). An end-member is not necessarily a species, but it may be. The term end-member, as used here, is

equivalent to the term 'constituent' used by Anderson and Crerar (1993). A set of end-members is independent if it is impossible to create any end-member in the set by linear combination of the other end-members.

The term proportion (p), is used to describe the relative quantity of any one end-member in an independent set of end-members, where $p_i = \frac{n_i}{\sum_j n_j}$; n_i is the number of moles of i, and $\sum p_i = 1$. The term 'apparent mole fraction' (x_{app}), is used to describe the relative quantities of the end-members which were present prior to mixing. For example, if 10 mol of NaCl were added to 90 mol of water, then the apparent mole fraction of NaCl would be 0.1, regardless of speciation. Mole fraction (x_i), is retained as the general term.

3. Standard states

The standard state of end-members for which data is derived from measurements of the pure substance (e.g., CO_2, H_2O, liquid NaCl), is that of unit activity of the pure end-member at the pressure and temperature of interest. The standard state of end-members for which thermodynamic data is derived from measurement of the properties of dilute solutions (e.g., aqueous $CaCl_2$) is a pure hypothetical standard state where $a_i \to 1$ as $x_i \to 1$ (Raoults Law) at any pressure and temperature. This standard state has a unit mole fraction of the end-member, but in other respects has the properties of the solute in infinitely dilute solution (Stokes, 1991). Thus, this standard state must always be hypothetical. Relationships between standard state chemical potentials for the mole fraction and molal concentration scales are discussed and illustrated in Appendix A (see also Stokes, 1991).

4. Formulation

The fluid is viewed as a loose framework of sites, each of which contains a solvent molecule, a charged solute ion, or an uncharged solute molecule. This approach is implicit in most existing activity models (e.g., Helgeson et al., 1981; Pitzer, 1973; Pitzer and Simonson, 1986). The Gibbs energy of the solution is

$$G_{\text{phase}} = \sum x_i \mu_i = \sum x_i \mu_i^{\ominus} + \sum x_i RT \ln a_i.$$
$$= \sum x_i \mu_i^{\ominus} + \sum x_i RT \ln a_{i,\text{id}} + \sum x_i RT \ln \gamma_i, \qquad (1)$$

where the sum is over an independent set of end-members. G is Gibbs energy, x_i is the proportion of end-member i, μ_i is the chemical potential of that end-member, $\mu_i^{\ominus}$ is the chemical potential of i at some standard state, a_i is the activity of i, $a_{i,\text{id}}$ is the ideal activity of end-member i, and γ_i is the activity coefficient for that end-member. All symbols are defined in Table 1. Here, the ideal activity accounts for the thermodynamic effects of mixing that would occur if there were no heat evolved on mixing and if the volume of the solution phase were equal to the sum of the volumes of its pure end-members before mixing. The non-ideal activity term accounts for other changes in the thermodynamics of solution that occur as a result of a solution composition different to that of the standard state. These effects include changes in hydrogen bonding, hydration of ions, and long range electrostatic interactions.

5. Choice of end-members

The Gibbs energy of a fluid phase Eq. (1) is calculated from the sum of the contributions of an independent set of end-members. It is possible to use any set of end-members that describe the system; these need not have physical reality, or be present in positive quantities (Thompson, 1982). The number of independent end-members for a given system is determined by the composition and speciation of the modelled solution. An independent end-member is required for each chemical component in the solution. Further independent end-members are necessary if speciation in solution is taken into account. An additional end-member is required for each variable that is required to describe the speciation of the solution (Holland and Powell, 1996a). The total number of independent end-members required to describe a phase is $n_c + n_{sp}$ (Holland and Powell, 1996b), where n_c is the number of chemical components, and n_{sp} is the number of variables required to describe speciation within the system. For example, if a solution contains NaCl, Na^+, Cl^-, and H_2O, then the set of end-members must reflect the two chemical components, NaCl and H_2O, and the dissociation of NaCl into Na^+ and Cl^-. This gives a total of three independent end-members. These may be NaCl, H_2O, and $Na^+ + Cl^-$ (referred to as NaCl±), see below, or NaCl–$(H_2O)_6$, H_2O, and NaCl±, or, indeed, any other combination of the components that comprise the solution.

5.1. End-members to represent charged species

It is not possible to define the chemical potential of individual charged species in the normal way because the Gibbs energy-derived definition of chemical potential (μ):

$$\mu_i = \left(\frac{\partial G}{\partial n_i}\right)_{n_{j(j\neq i)},P,T} \qquad (2)$$

requires that the composition of *all* end-members (n_l) except that of interest (n_i) be held constant during the differentiation of the Gibbs energy (G) of the solution. Addition of a single charged component causes electrical work to be done to produce a charged solution, and this work would have to be included in Eq. (2). The activity of charged species has been measured (e.g., Rodil and Vera, 2003; Wilczek-Vera et al., 2004) but it is difficult to incorporate these measurements into a rigorous thermodynamic framework. Traditionally, this issue has been resolved by the use of mean ionic functions (Stokes, 1991; Anderson and Crerar, 1993; Nordstrom and Munoz, 1994). This approach has

Table 1
Key to symbols used in the text

Symbol	Quantity	Units
$\dot{a}$	Ionic radius	m
a_{id}	Ideal activity	—
app	Referring to apparent composition	Subscript
A_x	Debye–Hückel constant (mole fraction scale)	—
B_x	Debye–Hückel constant (mole fraction scale)	—
b,c,d	Stoichiometric coefficients	—
e_{o}	Charge on electron	Coulombs
ex	Excess	Subscript
G	Gibbs energy	kJ mol^{-1} or J mol^{-1}
id	Refers to ideal mixing	Subscript
i, j, ℓ	Solution components	Subscript
I_{diff}	Interval over which ionic strength approaches maximum	—
I_{L}	Maximum ionic strength for Debye–Hückel in mole fraction units	—
I_x	Ionic strength in mole fraction units	—
k	Boltzmanns constant	J mol^{-1}
k_{o}	cgs to kmg charge conversion	Farads m^{-1}
LRI	Long range interaction	superscript
m	Superscript referring to molal concentration scale	—
N_{A}	Avogadro's number	Molecules mol^{-1}
mix	Refers to chemical effects of mixing	Subscript
n_{s}	Number of solvent end-members	—
n_i	Mumber of moles of i	—
P	Pressure	GPa
p	Proportion	—
R	Gas constant	kJ mol^{-1} K^{-1}
T	Temperature	K
V	Molal volume of solution	m^3 mol^{-1}
VL	Van Laar	Subscript
W^*_{ij}	Size parameter adjusted interaction energy	kJ mol^{-1}
w_{ij}	Interaction energy	kJ mol^{-1}
x	Refers to mole fraction concentration scale	Superscript
x_i	Mole fraction of i	—
z_i	Number of charges on ion i	—
α	Size parameter	—
ε	Dielectric constant	—
ϕ	Size parameter adjusted proportion	—
γ	Activity coefficient	—
κ	Debye–Hückel inverse length	m^{-1}
μ_i	Chemical potential	kJ mol^{-1}
$\mu_i^{\ominus}$	Standard state chemical potential of i	kJ mol^{-1}
π	Pi (3.142...)	—
$\pm$	Subscript or postscript referring to mean compounds	—

—, indicates dimensionless constant or variable.

the advantages that it accounts correctly for the Gibbs energy associated with ideal mixing, and removes the necessity for an explicit charge balance requirement. Here, mean compounds are used as independent end-members for the purposes of thermodynamic description. They are distinguished from real neutral end-members by a $\pm$ addition to the formulae, e.g., NaCl$\pm$.

Mean chemical potentials, mean standard state chemical potentials, mean activities and mean activity coefficients for the mean ionic end-member $A_bC_d\pm_{\frac{1}{b+d}}$ are given by:

$$\mu_{A_bC_d\pm} = \frac{b\mu_{A^{b+}} + d\mu_{C^{d-}}}{b+d} \tag{3}$$

$$\mu^{\ominus}_{A_bC_d\pm} = \frac{b\mu^{\ominus}_{A^{b+}} + d\mu^{\ominus}_{C^{d-}}}{b+d} \tag{4}$$

$$a_{\mathrm{id},A_bC_d\pm} = x_{A^{b+}}^{\frac{b}{b+d}} x_{C^{d-}}^{\frac{d}{b+d}} \tag{5}$$

$$\gamma_{A_bC_d\pm} = \gamma_{A^{b+}}^{\frac{b}{b+d}} \gamma_{C^{d-}}^{\frac{d}{b+d}}. \tag{6}$$

respectively, e.g., Nordstrom and Munoz (1994). The stoichiometry of the mean end-members is defined so that one mole of a mean ionic compound gives one mole of ions in solution, i.e., $A_bC_d \Longleftrightarrow (b+d)A_bC_d\pm_{\frac{1}{b+d}}$. This gives the correct number of entities present in the solution and so allows mole fractions to be calculated correctly. The subscript$_{\frac{1}{b+d}}$ is dropped from this point onwards, for convenience. So, for example, dissolution and complete dissociation of one mole of $CaCl_2$ would give three moles of $CaCl_2\pm$.

The number of mean compounds for any solution is determined by the number of species present in solution,

and is $n_a + n_{cat} - 1$, where n_a is the number of anions and n_{cat} is the number of cations. However, the choice of the formulae of the mean compounds is flexible. For example, a solution that contains K^+, Na^+, $MgOH^+$, OH^-, SO_4^{2-} and Cl^-, can be defined by five mean compounds. One possibility would be KOH±, K_2SO_4±, KCl±, NaOH± and MgOHOH±. Another would be NaCl±, Na_2SO_4±, NaOH±, KCl±, and MgOHCl±.

Problems with the common ion effect are avoided because the ideal activity and the activity coefficient of mean end-members that contain a given ion are functions of the concentration of that ion in solution. The concentration of the ion is itself a function of the proportions of *all* the end-members that contain that ion. This is reflected by the definitions of ideal activity and the activity coefficient, which may include the proportions of several end-members. This means that the proportion of a mean compound that contains a common ion is not equal to its ideal activity (see Eq. (5)), and that any one ion may be distributed between several mean compounds. Care should be taken with this facet of the use of mean compounds because it differs slightly from that used in other applications (e.g., Nordstrom and Munoz, 1994).

6. Ideal activity

If an end-member is a real entity in solution then, for this conceptual solution model, the ideal activity of that end-member is its proportion ($a_{i,id} = x_i$; Powell, 1978). If the end-member is hypothetical then the ideal activity is a more complicated function of composition, as in the case of end-members that represent charged species discussed above. Hydration and formation of polymolecular complexes can be incorporated into the ideal activity term. This can be accomplished via the use of end-members with the stoichiometry of the chosen species. For example, if the end-members of a SiO_2–H_2O solution are defined to be $SiO_2{\cdot}4H_2O$ and H_2O then the ideal activities of the end-members are $\frac{x_{SiO_2,app}}{1-4x_{SiO_2,app}}$ and $\frac{x_{H_2O,app}-4x_{SiO_2,app}}{1-4x_{SiO_2,app}}$, respectively, where the subscript $_{app}$ refers to apparent mole fractions. Alternatively, the ideal activity could be defined as a more complicated function of compositional and speciation variables (Holland and Powell, 1996a,b). However, the choice is restricted by the choice of compounds for which a standard state potential is known.

7. Non-ideal activity: the DH–ASF model

The excess energy of mixing (G_{ex}) is split into two components. The first accounts for the effects of long range electrostatic interactions (G_{ex}^{LRI}), and is represented by the Debye–Hückel expressions described below. The second, Van Laar, term (G_{ex}^{VL}) accounts for all other interactions.

$$G_{ex} = G_{ex}^{LRI} + G_{ex}^{VL} = RT \ln \sum p_i \ln \gamma_i^{LRI} + RT \ln \sum p_i \ln \gamma_i^{VL} \quad (7)$$

This approach follows that of Helgeson et al. (1981) and Li et al. (1994), among others. The Debye–Hückel and Van Laar expressions were both developed to represent physical processes that are known to occur in solutions; long range electrostatic interactions, in the case of Debye–Hückel, and shorter range pairwise interactions, in the case of Van Laar. The parameters involved in the use of these equations may therefore be expected to have a physical meaning. However, the Van Laar parameters are used here to represent a range of processes that lead to non-ideality and so the model is semi-empirical. Nevertheless, information on the nature of the processes that lead to non-ideality may be obtained from the parameters, as discussed below.

7.1. Long range interactions: Debye–Hückel term

An extended Debye–Hückel term is used to describe long range interactions in dilute solutions, and as a contribution towards the activity coefficient in more concentrated solutions. The Debye–Hückel expression defines a Helmholtz energy (non-ideal energy at constant T and V) rather than a Gibbs energy (non-ideal energy at constant T and P), but the two quantities are equivalent if the PV work performed by long range electrostatic interactions is assumed to be negligible (c.f. Davidson, 1962; Cabezas and O'Connell, 1993). This assumption is made here.

The expression used here is similar to commonly used Debye–Hückel expressions, but it was derived to deal with mixed solvent solutions, following the principles outlined in Davidson (1962) and the approach described by O'Connell (2003). An additional adaptation has been made so the expression can be applied to concentrated solutions. Terms in the Debye–Hückel expression that depend on the solvent, such as dielectric constant, solution volume, and molal mass, become functions of solvent composition. This is similar to the approach followed by Akinfiev and Zotov (1999), but the expression used here incorporates the solvent dependency of molal mass as well as solvent-related changes in dielectric constant. Differentiation of solution energy to obtain activity coefficients was performed under the assumption that solvent chemical potentials could be affected by changes in the number of moles of solute (see discussion in Cabezas and O'Connell, 1993). This treatment results in Debye–Hückel expressions that obey the Gibbs–Duhem relationship. Versions of Debye–Hückel that do not provide an expression for the activity coefficient of the solvent contravene the Gibbs–Duhem relationship. The maximum value of the contribution of the Debye–Hückel term is set to that made by a solution with an ionic strength equivalent to 0.1 molal. The use of this arbitrary limit eliminates computational artefacts that arise from application of the Debye–Hückel equation outside its valid compositional range and allows the expression to deal with more concentrated solutions than those for which the expression was originally derived. The Debye–Huckel function is rendered continuous by the use of a transform on the ionic strength, such that the ionic strength input into

the Debye–Huckel equation, $I_{x,\mathrm{DH}}$, varies smoothly to a maximum of 0.1 molal Eq. (8).

$$I_{x,\mathrm{DH}} = I_x + \frac{(I_\mathrm{L} - I_x)(\mathrm{Erf}[(1/I_\mathrm{diff})(I_x - I_\mathrm{L})] + 1)}{2} \tag{8}$$

where I_x is ionic strength, I_L is the chosen limit, and I_diff is the interval over which ionic strength approaches its limit. I_diff is set to 2×10^5 for the applications described here. The physical implication of this strategy is that long range ordering effects do not increase above a certain ionic strength; that is, the effects of short-range ordering screen ions from the Coulombic interactions that cause long range ordering at low solute concentrations. A consequence of the fixed maximum value is that the Debye–Hückel term is non-zero at a mole fraction of 1 and so the activity coefficient should be adjusted to maintain unit activity in the standard state. However, this correction cancels against the Debye–Hückel term in the shift between molal and mole fractions standard states (see Appendix A) and so both may be omitted.

The Debye–Hückel expressions for the activity coefficient for solvents, $\gamma_{k,\mathrm{sv}}$, and the mean ionic form of solutes, $\gamma_{j\pm,\mathrm{sl}}$, are

$$\ln\gamma_{k,\mathrm{sv}} = \frac{V_\mathrm{sv}\kappa^3}{8\pi N_\mathrm{A}}\sigma \tag{9}$$

and

$$\ln\gamma_{j\pm,\mathrm{sl}} = -\frac{k_\mathrm{o}e_\mathrm{o}^2|z^+z^-|}{2\varepsilon kT}\left(\frac{\kappa}{1+\kappa\dot{a}}\right) = -\frac{|z^+z^-|A_x\sqrt{I_x}}{1+\dot{a}B_x\sqrt{I_x}} \tag{10}$$

respectively (O'Connell, 2003). V_sv is the molal volume of the solvent, k is Boltzmann's constant (J K^{-1}), N_A is Avogadro's constant, T is the temperature in Kelvin, e_o is the charge on an electron, ε is the dielectric constant, I_x is the mole fraction scale ionic strength ($\sum_i \frac{1}{2}z_i^2x_i$), and takes a maximum value of 0.0018, equivalent to a molal ionic strength of 0.1. k_o is the constant for conversion between cgs and kmg charge units ($\frac{1}{4\pi\varepsilon_o}$), where ε_o is the permittivity of a vacuum. z^+ and z^- are the positive and negative charges present on ions in the mean compound. $\dot{a}$ is the ion size parameter (m), which is taken here to be the same for all ions in solution (4.5×10^{-10} m): it is accepted that this is not appropriate for all ions in the solution, but the simplification is necessary to facilitate derivation of the expressions. The effects of this assumption on results is minimal. κ is the Debye–Hückel inverse length (m^{-1}), where

$$\kappa^2 = \frac{8N_\mathrm{A}\pi e_\mathrm{o}^2k_\mathrm{o}I_x}{kV\varepsilon T}. \tag{11}$$

V is the molal volume of solution, and σ is a function of κ and $\dot{a}$ given by

$$\sigma = \frac{3}{(\kappa\dot{a})^3}[1+\kappa\dot{a} - \frac{1}{1+\kappa\dot{a}} - 2\ln(1+\kappa\dot{a})] \tag{12}$$

A and B are the Debye–Hückel parameters.

$$A_x = \frac{k_\mathrm{o}e_\mathrm{o}^2\kappa}{2\varepsilon kT\sqrt{I_x}} \tag{13}$$

$$B_x = \frac{\kappa}{\sqrt{I_x}} \tag{14}$$

Values of A_x and B_x for $X(CO_2)$ values of 0, 0.1 and 0.2 are summarised in Appendix B. Symbols and constants are summarised in Table 1.

7.2. Other interactions: Van Laar

The Van Laar used here is the reformulation (Holland and Powell, 2003) of the original Van Laar model (Van Laar, 1906; Prausnitz et al., 1986), termed the asymmetric formalism (ASF). The value of the reformulation lies in its capacity to describe multi-component solutions in a computationally tractable way. The ASF model has been shown to represent the characteristics of mixing in ternary feldspars, Ca–Mg carbonates, H_2O–CO_2 mixtures, simple silicate melts (Holland and Powell, 2003) and amphiboles (Dale et al., 2005). The ASF is the sum of binary contributions made by pairwise interactions between end-members in the independent set:

$$RT\ln\gamma_\ell^\mathrm{VL} = -\sum_{i=1}^{n-1}\sum_{j>i}^{n} q_iq_jW_{ij}^*, \tag{15}$$

where $q_i = 1-\phi_i$ if $i=\ell$ and $q_i = -\phi_i$ otherwise. ϕ_i is a weighted function of the proportions of the end-members, p_i.

$$\phi_i = \frac{p_i\alpha_i}{\sum_j p_j\alpha_j}. \tag{16}$$

The ϕ_i are proportions weighted with α parameters, where the α parameters control the asymmetry of the interaction. The sign and magnitude of each term in Eq. (15) is determined by the W_{ij}^* parameter.

$$W_{ij}^* = w_{ij}\frac{2\alpha_l}{\alpha_i+\alpha_j}, \tag{17}$$

which is a function of interaction energy w_{ij}, and the relative sizes of the relevant α parameters. The α of l, the end-member of interest, scales the W_{ij}^* parameter so that W_{ij}^* depends on the properties of the end-member l as well as those of i and j. The W_{ij}^* terms incorporate all mixing energies between pairs of end-members; it includes energies associated with hydration, electrostriction and solvent structure collapse. ASF becomes equivalent to a symmetric model, e.g., symmetric formalism (Powell and Holland, 1993) when all the α parameters are equal. The same formulation applies to both ions and solvent. It is necessary to correct solute chemical potentials with a $\gamma_{x_i}=0$ term in cases where the original data is referenced to infinite dilution (See Appendix A for discussion of molal-mole fraction conversion). This step may be undertaken most conveniently in the calculation of the standard state chemical potential. An example of calculation of chemical

potentials for end-members in the system NaCl–H_2O is given in Appendix C.

8. Model application

8.1. Parameterisation

The thermodynamics of mixing are most sensitive to the parameters that are associated with end-members that have large ϕ values. Large ϕ values are calculated for end-members that are present in large quantities, or that have a disproportionately large α Eq. (16). Mixing between end-members with small ϕ values makes a relatively small contribution to the total energy of solution.

8.2. α Terms

The relative sizes of the α terms determine the asymmetry of the binary interaction energies (Fig. 1). If they are identical then the Van Laar-related excess energy attributed to the pair is symmetrical; if not then the excess energy is skewed towards the end-member with the smaller α. An increase in α results in an increase in the non-ideal activity terms for solutions where the end-member is dilute (Fig. 1).

Some previous applications of Van Laar (e.g., Prausnitz et al., 1986; Holland and Powell, 2003) have used molal volumes, or ratios of molal volumes, for the α terms, with some success. The physical interpretation of this substitution is that asymmetry in non-ideal interactions results from the juxtaposition of molecules of different sizes. This approach is unlikely to be successful for aqueous solutions because asymmetry in the non-ideality stems from parameters in addition to ion size, such as polarity. Therefore α parameters are treated as adjustable and are allowed to vary as a function of pressure and temperature. However, the physical size of the species represented by an end-member is considered to be a major influence on non-ideality, and so the size of α is expected to correlate approximately with the size of the species in solution that the end-member describes. α_i values are always combined in ratios Eq. (17), so only $n-1$ of the α values in a system containing n end-members are independent. The α of water is set to 1 in all cases.

A number of studies (e.g., Anderson et al., 1991; Shock et al., 1992; Caciagli and Manning, 2003) have noted that certain aspects of the behaviour of aqueous solutions, which include the extent of non-ideality, are related to the density of water. Trials were therefore made in which α values were linked to the density of water via the relationship $\alpha_i = \frac{\alpha'_i}{V_{H_2O}}$. Values of α that were derived in this way were much less sensitive to pressure and temperature than density-independent values of α, so this approach was adopted. The relationship between α and water density would be expected to break down in solutions where $X(H_2O)$ becomes small, and the approach should be abandoned in such circumstances. However, solutions of geological interest that fall into this category are relatively rare, and so the relationship is retained.

8.2.1. w_{ij} terms

The size and sign of the w_{ij} terms determine the sign and magnitude of the binary contributions towards the overall excess energy of mixing (Fig. 1), although the α parameters also affect the size of the terms: see Eq. (17). A positive interaction energy between two end-members indicates that mixing is inhibited in comparison to ideal mixing, whereas

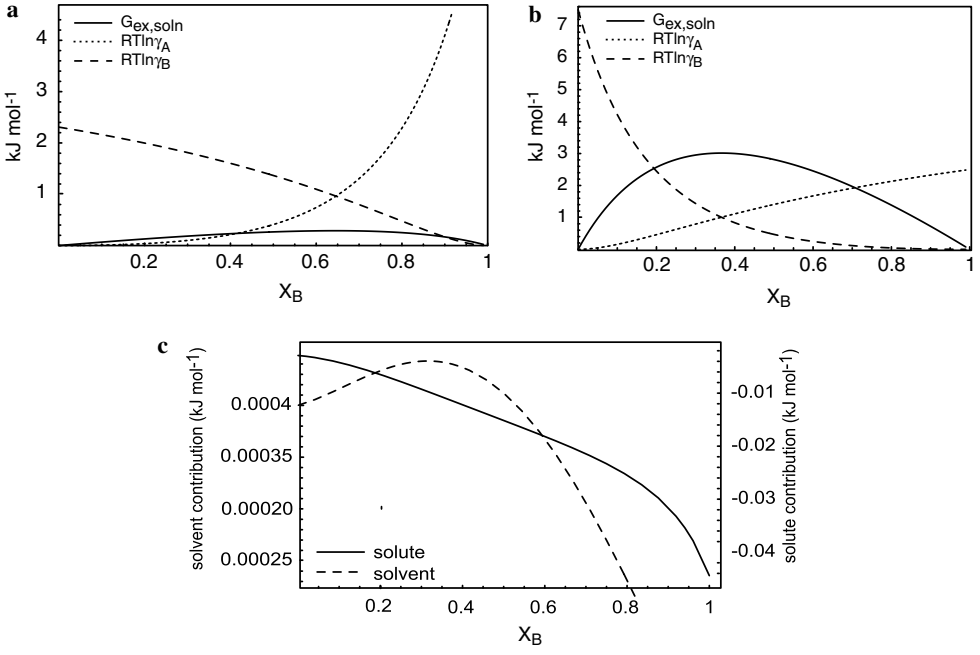

Fig. 1. $RT\ln\gamma$ and G_{ex} for binary solution. (a) VL contribution: $\alpha_A = 1$; $\alpha_B = 0.3$; $w_{AB} = 5$; (b) VL contribution: $\alpha_A = 1$; $\alpha_B = 3$; $w_{AB} = 5$; (c) Debye–Hückel contribution ($p_i RT \ln \gamma_i^{LRI}$) for solvent and solute interactions at 0.5 GPa, 873 K, and for $p_{solute} = 0.0018$. Note second x axis for the solute contribution.

a negative interaction energy indicates that mixing is energetically favourable. The terms of the derivation of Eq. (15) do not allow w_{ij} to vary as a function of composition, although w_{ij} may vary as a function of temperature and pressure. Temperature-dependence of w_{ij} implies that the term accounts for entropy of mixing that is not dealt with by the ideal mixing term ($\frac{\partial G_{ex}}{\partial T} = -S_{ex}$). Pressure-dependence of w_{ij} implies that the excess volume of mixing is significant ($\frac{\partial G_{ex}}{\partial P} = V_{ex}$). Drastic changes in the P or T dependence of the w_{ij} parameters would suggest that the systematics of mixing alter in a way that is not provided for by the ideal mixing model.

8.2.2. Calibration

The small number of experimental data points that are available for the systems of interest mean that it is difficult to constrain P or T dependencies of the α or w_{ij} parameters. Calibrations were therefore made, where possible, under the assumption that the α and w_{ij} parameters were independent of P and T. It is necessary to specify $n-1$ α parameters and $\frac{n(n-1)}{2}$ w_{ij} parameters to model a solution that contains n end-members. This is a smaller number than that required for activity models that use ternary interaction parameters or composition-dependent binary virial terms, but the number can still be inconveniently large. It may therefore be acceptable to neglect the solute-solute terms in Eq. (15) (i.e., solute w_{ij} values are set to zero), in cases where the data available is not sufficient to constrain all parameters. This is possible when the solute mole fractions are small because solute–solute mixing terms contribute only a small amount to the overall Gibbs energy of mixing. If these terms are neglected then the total number of parameters required to describe a solution that contains n end-members, of which n_s are solvent end-members, and in which the non-ideal mixing is not P- or T-dependent, is $\frac{n_s}{2}(2n - n_s - 1)$. P and T dependencies of α and/or w_{ij} will increase this figure.

The parameters used in the calculations that are discussed in the examples below were obtained by manual manipulation of the ASF parameters to minimise a least-square diagnostic. Least-squares, robust (e.g., Powell et al., 2002) and non-linear fitting routines did not prove any more successful than this technique. The fits are subject to possible multiple minima. However, standard deviations are close to experimental error so the fits can be considered to be successful. Debye–Hückel parameters depend only on the mole fractions of the solvent end-members, pressure and temperature, and so do not require calibration.

8.2.3. Implementation

The model has been coded to run within THERMOCALC 3.25, a computer program that calculates equilibria for systems containing complex solid, silicate liquid, and aqueous solutions (Powell et al., 1998; White et al., 2001). Standard state chemical potentials for aqueous end-members are calculated with a modified form (Holland and Powell, 1998) of the Andersen Density Model equation of state (Anderson et al., 1991). The standard state thermodynamic parameters are tabulated in Holland and Powell (1998). The code allows α and w_{ij} to vary as linear functions of P and T: $\alpha = a_\alpha + b_\alpha T + c_\alpha P$ and $w_{ij} = a_w + b_w T + c_w P$, respectively, although this facility is not utilised for most of the examples described below.

The dielectric constant of H_2O–CO_2 solutions is calculated after Akinfiev and Zotov (1999), using the Archer and Wang (1990) formulation for the dielectric constant of pure water and a modified version of the Kirkwood equation (Kirkwood, 1939) to account for mixing with CO_2. Volumetric properties of H_2O–CO_2 mixtures are calculated using a modified Redlich–Kwong equations of state for H_2O and CO_2 and an asymmetric Van Laar mixing model, see Holland and Powell (2003) for more details. The contribution of other solution end-members present in large quantities, such as NaCl, could usefully be incorporated into the calculation of volume and dielectric constant, but this is not performed here. This omission is justified by the small size of the Debye–Hückel term relative to other contributions to the chemical potential (Fig. 1c). The value of the Debye–Hückel term depends on ionic strength, which is itself a function of the speciation, so an iterative solution is used to calculate this contribution to the activity. Activity–composition relationships were specified using intermediate composition and speciation variables, as described in Powell et al. (1998).

9. Calibration and application

The model was calibrated with experimental data available for the systems NaCl–H_2O (Koster van Groos, 1991; Aranovich and Newton, 1996); KCl–H_2O (Aranovich and Newton, 1997); NaCl–SiO_2–H_2O (Newton and Manning, 2000; Shmulovich et al., 2001), H_2O–CO_2–SiO_2 (Newton and Manning, 2000; Shmulovich et al., 2001), and albite–H_2O (Shen and Keppler, 1997; Stalder et al., 2000). The calibrated parameters are then used to investigate the effect of the presence of saline fluids in the system CaO–MgO–SiO_2–CO_2–H_2O–NaCl. These systems were chosen because experimental data is available over a relatively wide range of pressure, temperature and fluid compositions, and because the chemical components of these systems are abundant in geological fluids. The calibrated parameters are summarised in Table 2.

9.1. Calibration: NaCl–H_2O

The halite–water binary exhibits complete mixing at pressures of more than 0.2 GPa and at temperatures above the halite melting point. At lower temperatures the system comprises solid halite and a one phase fluid. At around 0.2 GPa NaCl is thought to be almost completely associated (Aranovich and Newton, 1996), and the characteristics of the system can be represented by ideal mixing between associated salt and water. The degree of dissociation increases with increasing pressure (Aranovich and Newton,

Table 2
Summary of parameters used to calculate Figs. 2, and 4–7

P (GPa)	T (°C)	i	j	w_{ij}	α'_i	α'_j	x_{H_2O} range	Figures
0.2–0.7	500–900	hltL	H_2O	3	0.5	V_{H_2O}	0.1–0.9	2
0.2–0.7	500–900	NaCl±	H_2O	−20	9	V_{H_2O}	0.1–0.9	2
0.2–1	600–900	syvL	H_2O	8	0.2	V_{H_2O}	0.6–0.95	4
0.2–1	600–900	KCl±	H_2O	−35	1	V_{H_2O}	0.6–0.95	4
1	500–900	aqSi	H_2O	0	1	V_{H_2O}	0.5–0.999	5A
1	500–900	aqSi	hltL	90	1	0.5	0.5–0.999	5A
1	500–900	aqSi	NaCl±	60	1	9	0.5–0.999	5A
0.435	700	aqSi	hltL	85	1	0.5	0.5–0.999	5B
0.435	700	aqSi	NaCl±	−45	1	9	0.5–0.999	5B
1	800	aqSi	CO_2	80	1	V_{CO_2}	0.5–0.999	5C
1.2–1.5	640–740	abL	H_2OL	2390-2.6T	8	1	0.7–1	7
1.2–1.5	640–740	abL	H_2O	1669-1.8T	1	1	0.7–1	7
0.05–2	400–1000	H_2O	CO_2	10.5 $\frac{V_{H_2O}+V_{CO_2}}{V_{H_2O}V_{CO_2}}$	V_{H_2O}	V_{CO_2}	0–1	5C

α' values are related to α by $\alpha_i = \frac{\alpha'_i}{V_{H_2O}}$ at the pressure and temperature of interest.

1996) and the representation of mixing becomes more complicated.

The activity model described above was used to calculate the halite saturation curve for the NaCl–H_2O system, and the brucite–periclase dehydration reaction in NaCl–H_2O–MgO (Fig. 2a). It was assumed that MgO did not enter the fluid phase. The fluid was described in terms of three end-members: water; associated NaCl with the properties of liquid NaCl (hltL); and dissociated NaCl with properties extrapolated from the 1 molal standard state (NaCl±). Trials were made using solutions that contained an additional end-member, $NaCl^0$, which is associated NaCl extrapolated from the 1 molal standard state. This did not produce a better fit to the data than the simpler model, which was therefore preferred. The results compare well with experimental data from Koster van Groos (1991) and Aranovich and Newton (1996): Fig. 2. Note that the x axis in Fig. 2 represents the apparent mole fraction of H_2O.

Four adjustable parameters (Table 2) were sufficient to describe the system:

$$w_{\mathrm{hltLH_2O}} = 3 \text{ kJ mol}^{-1}$$
$$w_{\mathrm{NaCl\pm H_2O}} = -20 \text{ kJ mol}^{-1}$$
$$\alpha'_{\mathrm{hltL}} = 0.5$$
$$\alpha'_{\mathrm{NaCl\pm}} = 9$$

The standard deviation of the residuals between predicted and measured $x_{H_2O,app}$ are 8, 11 and 21 °C at 0.2, 0.42 and 0.7 GPa, respectively. This is close to experimental uncertainty, when compositional uncertainties are taken into account. The degree of dissociation was predicted to increase with increasing pressure (Fig. 2b), as proposed by Aranovich and Newton (1996) although the predicted decrease in association is less than that suggested by these authors. The pressure dependence of the data is modelled successfully in spite of the lack of any explicit pressure dependency for the α and w_{ij} parameters. This is attributed to the use of the density of water as a scaling factor for the α parameters (Section 8). The Aranovich and Newton activity–composition model (Aranovich and Newton, 1996) is based on the assumption that speciation is not dependent on fluid composition. Speciation is a relatively constant function of fluid composition in the region of

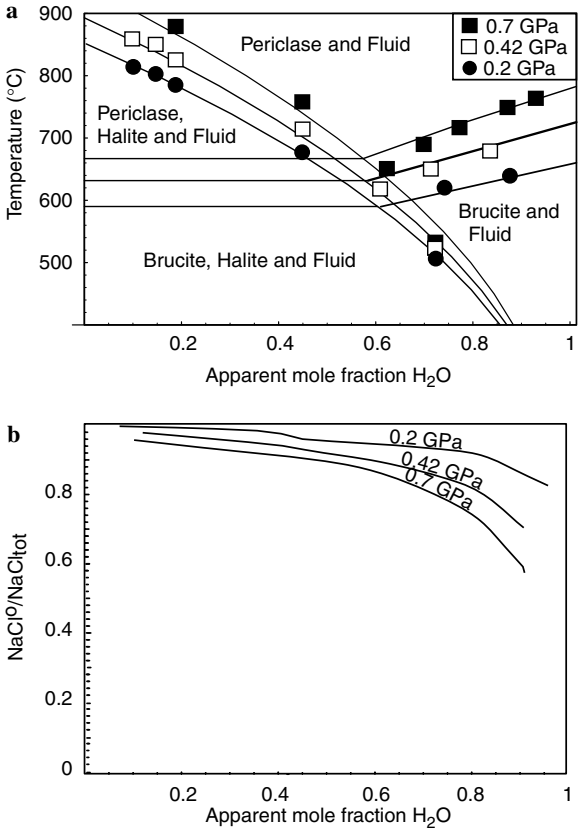

Fig. 2. (a)Comparison of experimental results from Aranovich and Newton (1996), and Koster van Groos (1991) (points) for the system NaCl–H_2O, with predictions made using DH–ASF model (lines). The same parameters are used for all calculations. Experimental errors are of the same magnitude as the standard deviation of the points from the line. (b) Predicted degree of dissociation for NaCl–H_2O solutions at the periclase–brucite or halite–liquid equilibria. The degree of association decreases with increasing pressure, and decreases sharply at high water mole fractions. This is consistent with qualitative predictions and the experimental results of Aranovich and Newton (1996). The kink occurs where the brucite–periclase and halite–fluid curves intersect.

the Aranovich and Newton dataset; this validates their approach. However, significant decrease in association is predicted in water-rich fluids. This is consistent with the arguments of Oelkers and Helgeson (1990). The predicted proportion of dissociated NaCl is consistent with trends shown by the results of molecular simulations (Sherman and Collings, 2002).

The parameters for NaCl± are consistent with current knowledge of NaCl-bearing aqueous solutions; the large α' and negative $w_{NaCl\pm,H_2O}$ reflect the large size of hydrated charged ions and the affinity of charged ions for aqueous solutions respectively. The broad range of pressure and temperature which are fit successfully with only four adjustable parameters suggests that the conceptual model is appropriate.

The calibration was tested by application to the data of Tropper and Manning (2004). These authors investigated the equilibrium paragonite = jadeite + kyanite + H_2O in the presence of H_2O–NaCl fluids at 1.5 to 2.2 GPa and 700 °C. The DH–ASF model was used to calculate the position of this equilibrium and the results were compared to the experimental data (Fig. 3). The calibrated parameters for 0.2 to 0.7 GPa were used. The model agrees reasonably well with the data for the paragonite = jadeite + kyanite + H_2O reaction, with discrepancies of less than 0.1 GPa. However, the position of the albite + corundum + H_2O = paragonite reaction lies around 0.2 GPa lower than the experimental points. This is attributed to decreased accuracy of the calibration at low $X(H_2O)$ and pressures far from that of the calibration.

9.2. Calibration: KCl–H_2O

The characteristics of the KCl–H_2O system are similar to those of NaCl–H_2O. A single phase fluid, or fluid plus solid salt is stable across the entire compositional range at high pressure. Previous work (Aranovich and Newton, 1997) has also observed similarities in the systematics of association, with high pressures favouring the dissociated form.

The KCl–H_2O system was modelled in a similar way to that described for NaCl–H_2O (Fig. 4a). The end-members considered were sylvite liquid (syvL), water, and dissociated KCl extrapolated from the 1 molal standard state (KCl±). The data points of Aranovich and Newton (1997) are also shown. The parameters used to describe the system (Table 2) are

$$w_{syvLH_2O} = 8 \text{ kJ mol}^{-1}$$
$$w_{KCl\pm H_2O} = -35 \text{ kJ mol}^{-1}$$
$$\alpha'_{syvL} = 0.2$$
$$\alpha'_{KCl\pm} = 1$$

The standard deviation of the residuals between the experimental and modelled data was less than 15 °C. This is similar to the uncertainties associated with the experimental data. The degree of dissociation increases with pressure (Fig. 4b), as for NaCl. Parameters are similar to those for NaCl, which is to be expected given the similar properties of Na and K. The physical interpretations of the parameters are also generally consistent with expectations.

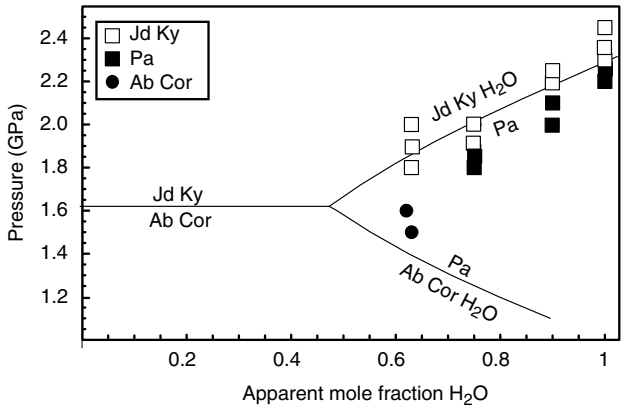

Fig. 3. Comparison of experimental results (points) from Tropper and Manning (2004) with predictions based on the DH–ASF model (lines). Calibration parameters were those obtained for 0.2 to 0.7 GPa. The model performs reasonably well at high $X(H_2O)$ in spite of the extrapolation to higher pressures, but the position of the albite+corundum+H_2O = paragonite equilibrium is underestimated by around 0.2 GPa.

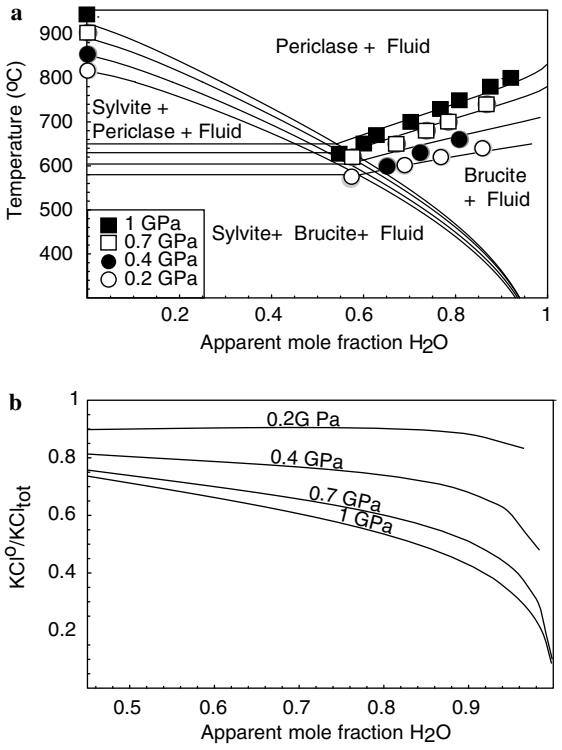

Fig. 4. (a) Comparison of experimental results for the system KCl–H_2O from Aranovich and Newton, 1997 (points) with predictions made using DH–ASF model (lines). The same parameters are used for all calculations. Experimental errors are of the same magnitude as the standard deviation of the points from the line. (b) Predicted degree of dissociation for KCl–H_2O solutions at the periclase–brucite equilibria at 0.2, 0.4, 0.7, and 1 GPa.

SyvL and H_2O mix poorly, as indicated by the positive value of w_{syvLH_2O} and the negative $w_{KCl\pm H_2O}$ reflects the affinity of the charged ions for aqueous solution. The low value of $\alpha'_{KCl\pm}$ is somewhat surprising given the generally made assumption that hydrated ions are large. However, the parameters are less well constrained than those for NaCl because of the lack of data in the low $X_{H_2O,app}$ region. The values for $w_{KCl\pm H_2O}$ and w_{syvLH_2O} show an inverse correlation, so that similar, but slightly worse fits than that shown in Fig. 4a are obtained for a value of $w_{KCl\pm H_2O}$ of 4 and a w_{syvLH_2O} of −25. More data is required to reduce the uncertainties on the w and α parameters, however, the parameter set here fits the data adequately from 0.2 to 1 GPa and from 600 to 900 °C and is thus deemed satisfactory.

9.3. Calibration: $NaCl–SiO_2–H_2O$

NaCl, H_2O, and SiO_2 are ubiquitous in geological fluids. The system exhibits changes in SiO_2 solubility as a function of pressure. Increases in salt concentration lead to increases in silica solubility (salting-in) at pressures less than 0.2 GPa, whereas increases in salt concentration lead to decreases in quartz solubility (salting-out) at higher pressures; (Xie and Walther, 1993; Newton and Manning, 2000; Shmulovich et al., 2001).

The $NaCl–SiO_2–H_2O$ system comprises two binary systems for which data is available. Parameters for $NaCl–H_2O$ interactions were taken from the fit to experimental data in the binary system that is described above. Extrapolation of these parameters to pressures higher than 0.7 GPa is associated with some degradation of the fit; temperature residuals in the $NaCl–H_2O$ system increase from 21 °C at 0.7 GPa to 33 °C at 1 GPa, but this is still close to experimental uncertainty. $SiO_2–H_2O$ was investigated by Manning (1994); his data are consistent with ideal mixing between an aqueous silica end-member (aqSi) and water ($w_{SiO_2,H_2O} = 0, \alpha'_{SiO_2} = 1$), and these values are adopted here. This is supported by the low concentrations and neutral charge of the aqueous silica species, and by the ability of thermodynamic data derived using the assumption to replicate experimental data for $H_2O–SiO_2$ systems over a wide range of pressures and temperatures (not shown).

The $NaCl–H_2O–SiO_2$ system was modelled under the assumption that the aqueous solution comprises four independent end-members: H_2O; aqueous silica monomers (aqSi); associated NaCl with the properties of liquid NaCl; and dissociated NaCl (NaCl±). A comparison between the 1 GPa data of Newton and Manning (2000) and the modelled dependence of quartz solubility on NaCl concentration is shown in Fig. 5a. Additional parameters (Table 2) used were:

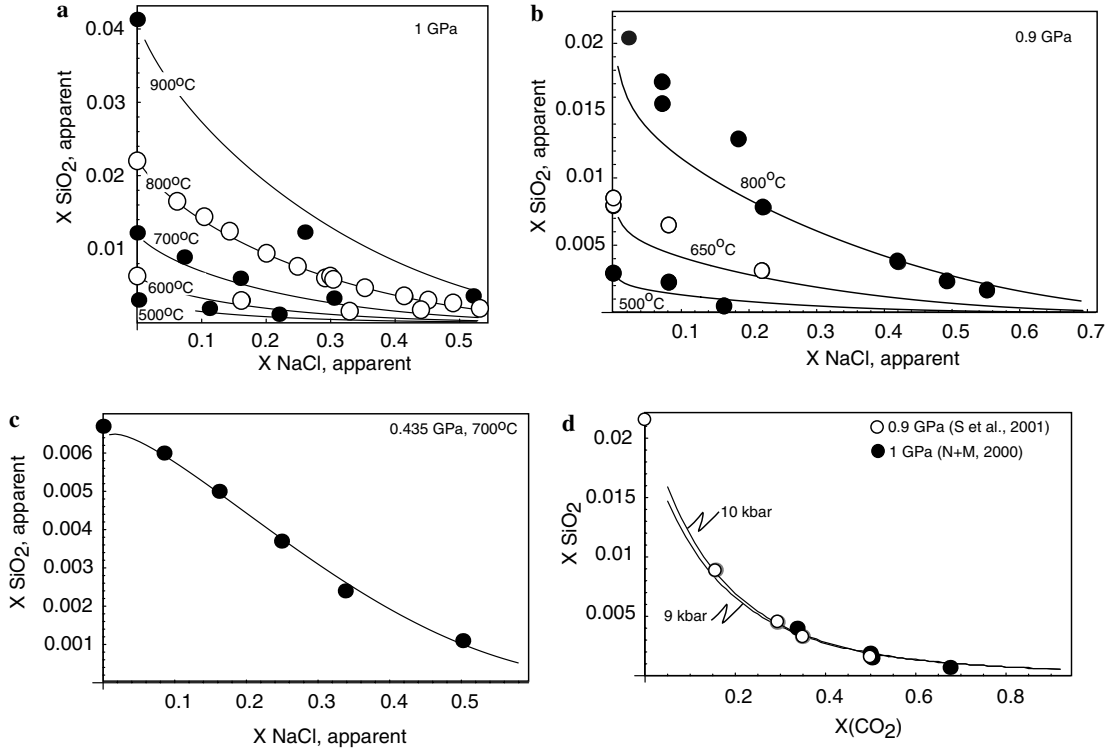

Fig. 5. Comparison of measurements of quartz solubility in (a, b, and c) saline and (d) CO_2-bearing solutions with predictions made using the ASF activity coefficient formulations. (a), $H_2O–SiO_2–NaCl$, 1 GPa, 500–900 °C; results from Newton and Manning (2000). (b) $H_2O–SiO_2–NaCl$, 0.9 GPa, 500–800 °C; results from Shmulovich et al. (2001). (c) $H_2O–SiO_2–NaCl$ at 700 °C, 0.435 GPa. Note the very different shape of the solubility curve: results from Newton and Manning (2000). (d) $H_2O–SiO_2–CO_2$ at 800 °C and 0.9 and 1 GPa. Results from Newton and Manning (2000) and Shmulovich et al. (2001).

$$w_{\mathrm{hltL,aqSi}} = 90 \text{ kJ mol}^{-1}$$

$$w_{\mathrm{NaCl\pm,aqSi}} = 60 \text{ kJ mol}^{-1}$$

The agreement between prediction and observation is good between 500 and 900 °C, and for aqueous silica solubilities between 0.11 and 2.2 molal. Positive values for the mixing energies between aqueous silica–hltL and aqueous silica–NaCl± are consistent with the disinclination of SiO_2 to dissolve in saline solutions and its consequent preference for an aqueous solvent, as proposed by Newton and Manning (2000). The parameters above were used to predict quartz solubility at 0.9 GPa, and the results were compared (Fig. 5b) to the data of Shmulovich et al. (2001). The model underpredicts quartz solubility at lower salt concentrations ($X_{\mathrm{NaCl}} < 0.2$) at 800 °C but agreement between prediction and experiment is good at other conditions. The difference between the predicted and observed solubilities may be attributed to inapplicability of the α parameters, or w_{ij} mixing energies at 0.9 GPa, or to systematic experimental error. More experimental data is required to differentiate between these possibilities.

Newton and Manning (2000) also present quartz solubilities at 0.2 and 0.435 GPa. The data at 0.2 GPa exhibits salting-in at low salt concentrations; this switches to salting-out as the salt concentration increases. The data at 0.435 GPa shows salting-out at all concentrations, but the shape of the solubility curve in $X(\mathrm{SiO_2}) - X(\mathrm{NaCl})$ space is convex, rather than concave as at the higher pressures (Fig. 5c). Prediction of quartz solubility at these lower pressures was attempted, using the activity model and the 1 GPa activity coefficient parameters that are tabulated above. If the speciation, excess volumes and excess enthalpies varied only as a function of density then the 1 GPa parameters should apply at this pressure, in the same way that the parameters for NaCl–H_2O may be extrapolated successfully between 0.2 and 1 GPa. However, this exercise did not predict the shape of the solubility curves correctly. Thus, one or more parts of the combination of ideal mixing model, α parameters, or w_{ij} mixing energies is not appropriate to describe the solution at these lower pressures. The pressure-dependency of the change suggests that there may be a change in the excess volume of mixing. This could be due to changes in the number of waters of hydration as suggested by Xie and Walther (1993), or to the presence of alkali-silica hydrous complexes e.g., Anderson and Burnham (1983). However, the data is so sparse that such proposals are merely speculative, although *P*-dependent changes in Si-speciation at pressures greater than 1 GPa have been confirmed (Zotov and Keppler, 2002). The 0.435 GPa data (Fig. 5c) can be fit with the parameters

$$w_{\mathrm{hltL,aqSi}} = 85 \text{ kJ mol}^{-1}$$

$$w_{\mathrm{NaCl\pm,aqSi}} = -45 \text{ kJ mol}^{-1}.$$

The change in sign for the parameter $w_{\mathrm{NaCl\pm,aqSi}}$ is difficult to interpret with the small quantity of data available. If the change in solution behaviour is due to some alteration in the systematics of solvation then this should be reflected in the ideal mixing model, rather than with compensatory changes in the *w* values, and so it is likely that this fit is empirical.

9.4. Calibration: silica concentration in CO_2-bearing solutions

CO_2 is common in geological solutions (e.g., Baker et al., 1991; Phillips and Powell, 1993; Ferry, 1994; Lowenstern, 2001). The solvation and speciation properties of CO_2 are different to those for H_2O, and thus its effect on solution characteristics can be significant. For example, addition of CO_2 to solution at high pressures (> 0.8 GPa) substantially reduces the solubility of SiO_2 (Newton and Manning, 2000; Shmulovich et al., 2001).

The system H_2O–CO_2–SiO_2 was modelled with an ideal mixing model for H_2O–SiO_2, as described above, and mixing parameters for H_2O–CO_2 taken from Holland and Powell (2003). End-members considered were H_2O, CO_2 and the aqueous silica monomer, aqSi (SiO_2). Solutions were assumed to be in equilibrium with pure quartz. Model results are compared with experimental SiO_2 solubilities (Newton and Manning, 2000) for the system (Fig. 5d) at 1 GPa. The additional parameter used to gain the fit (Table 2) is:

$$w_{\mathrm{CO_2,aqSi}} = 80 \text{ kJ mol}^{-1}$$

The standard deviation from the predicted values is, again, within experimental uncertainties. The calibration was tested by a comparison of the model results for 0.9 GPa with the experimental data of Shmulovich et al. (2001). The two lines, and the position of the data points, are almost identical for the two pressures, but nevertheless a good agreement is obtained. The large positive value for $w_{\mathrm{CO_2,aqSi}}$ reflects the disinclination of quartz to dissolve in a non-polar, non-aqueous solvent.

9.5. Calibration: co-existing silicate melt and aqueous fluids

The solubility of water in silicate melts, and the solubility of silicate constituents in aqueous fluids, increase as pressure and temperature increase. This trend has been shown to end in a second critical point for systems such as SiO_2–H_2O (Kennedy et al., 1962; Anderson and Burnham, 1965) and albite–H_2O (Paillat et al., 1992; Shen and Keppler, 1997; Stalder et al., 2000), with far-ranging implications for rheological, mineralogical and seismic properties in the lower crust and upper mantle. An advantage of the mole fraction concentration scale used by the DH–ASF model is that modelling of melt-fluid-rock interactions becomes possible.

The data of Shen and Keppler (1997) was used to calibrate DH–ASF parameters for fluid coexisting with melt in the system albite–H_2O. The melt was assumed to contain an albite liquid and a H_2O end-member with melt-like properties. Thermodynamic properties of the

H_2O end-member are given by White et al. (2001). The thermodynamics of mixing of the melt end-members is described by a symmetric formalism model (e.g., Powell and Holland, 1993), with one adjustable parameter, w_L. The fluid was also assumed to comprise two endmembers; an albite liquid with standard state thermodynamic properties identical to that of the albite liquid in the melt, and H_2O. Mixing thermodynamics for the fluid were represented by the DH–ASF model, which requires specification of a size parameter for albite, α_{abL} and energy of mixing between the two end-members, w_F. α_{abL} was set to 8.

The model replicates the data well (Fig. 6) on the sides of the solvus but does not predict fluid and melt compositions close to the top of the solvus. This is attributed to difficulties with the EOS, rather than to the mixing model, as thermodynamic properties are steep in the vicinity of critical points. Reasonable values for the compositions of liquid and fluid in equilibrium with albite are also predicted, although data for these pressures and temperatures in the *PT* plane of the section are unavailable for comparison. Data from Stalder et al. (2000) at pressures to 1.4 GPa and 700 °C are also within experimental error of values predicted by the model (not shown).

Parameters used were:

$$w_L = 2390.6 - 2.6T \text{ kJ mol}^{-1}$$

$$w_F = 1669.1 - 1.8T \text{ kJ mol}^{-1}$$

The negative coefficient that describes the temperature dependency of both the *w* parameters suggests that there are increases in the entropy of mixing that are not accounted for by the simple two end-member mixing model. These increases could be due to the formation of a variety of hydrated complexes, or melts with lower degrees of polymerisation than the melts from which the thermodynamic properties were derived. The relatively large temperature dependency suggests that these parameters should not be extrapolated to pressures and temperatures much different to those of the calibration. Nevertheless, this example demonstrates the power of the DH–ASF approach, although substantially more data is required before the model can reach its full potential.

9.6. Application: $CaO–MgO–SiO_2–CO_2–H_2O–NaCl$

The $CaO–MgO–SiO_2–CO_2–H_2O$ system has been used successfully to represent metamorphism of siliceous dolomites (e.g., Skippen, 1974; Trommsdorff and Connolly, 1990; Baker et al., 1991). The system has been studied in detail because it represents real siliceous dolomite rocks reasonably well and exhibits a number of reactions over the pressure and temperature ranges found in the upper crust. Fluid inclusion evidence suggests that siliceous dolomites interact with saline solutions during metamorphism (e.g., Crawford et al., 1979; Trommsdorff et al., 1985; Costagliola et al., 1999). Experimental and theoretical studies of $H_2O–CO_2–NaCl$ fluids have produced successful EOS such as that of Duan et al. (1995), but the effect of salinity on phase relations in CaMSCH has not been determined experimentally. Skippen and Trommsdorff (1986) produced a qualitative estimate of phase relations within the system, and Heinrich et al. (2004) used the EOS of Duan et al. (1995) to investigate immiscibility at pressures less than 0.5 GPa, but quantitative investigations of miscible supercritical fluids have not been performed.

THERMOCALC was used to calculate isobaric ($P = 0.5$ GPa) $T–X(CO_2)$ sections for $CaO–MgO–SiO_2–CO_2–H_2O–NaCl$, at fixed $x_{NaCl,tot}$ values of 0.05 and 0.1, and for $CaO–MgO–SiO_2–CO_2–H_2O$ (Fig. 7). $x_{NaCl,tot}$ of 0.1 is approximately equivalent to 20 wt percent NaCl in aqueous solution, and is typical of the higher salinity solutions observed in fluid inclusions found in regionally metamorphosed rocks (e.g., Costagliola et al., 1999). $x_{NaCl,tot}$ is the sum of the proportions of associated and dissociated NaCl ($p_{hltL} + p_{NaCl\pm}$). The fluid was assumed to comprise associated salt with the properties of liquid NaCl (hltL), dissociated salt (NaCl±), aqueous silica (aqSi), water and CO_2. Mineral phases considered were pure tremolite, diopside, talc, dolomite, wollastonite, quartz and calcite. Quartz, calcite and fluid were considered to be in excess. Parameters for the activity coefficient model were taken from Table 2. Dissolved Ca and Mg were not considered because these elements are known to be sparingly soluble at the pressures and temperatures of interest (Xie and Walther, 1993; Aranovich and Newton, 1996).

The basic geometry of the $T–X(CO_2)$ projection is unchanged by the addition of salt up to mole fractions of 0.1 (Fig. 7). The positions of reactions with steep slopes in $T–X(CO_2)$ space are also almost unaffected. Reactions with shallow slopes in $T–X(CO_2)$ space, on the other hand, show changes of up to 10 °C in the temperatures of reaction. This has implications for estimates of $X(CO_2)$, which can be made from the intersection between observed mineral equilibria (e.g., tr = di), and temperatures measured by other methods. It can be seen that NaCl-driven changes

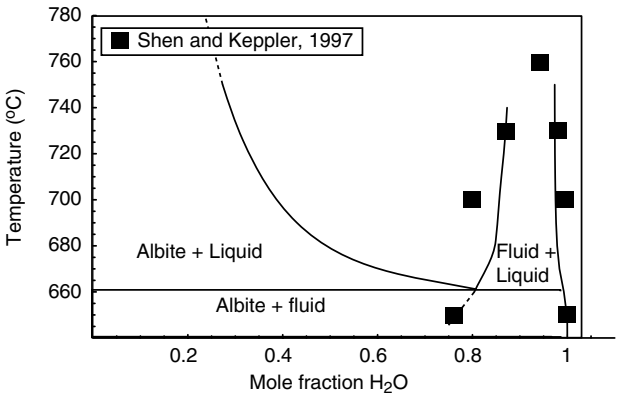

Fig. 6. $T–X(H_2O)$ section showing the fluid/melt solvus for albite–H_2O. Data points (squares) are from Shen and Keppler (1997). The lines are calculated with THERMOCALC. The diagram is polybaric; the points at 650 °C are at 1.22 GPa and the points at 760 °C the pressure is 1.45 GPa. Data points at the lowest temperatures are metastable.

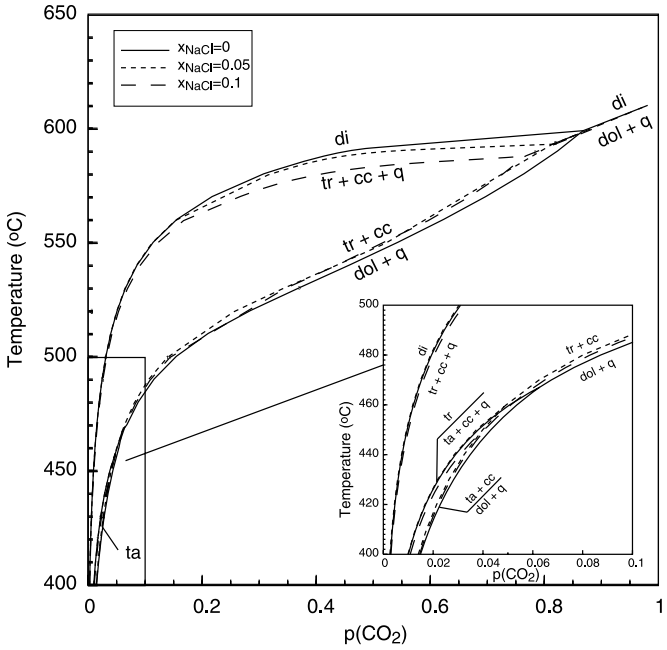

Fig. 7. Isobaric T–$X(CO_2)$ section for CaMSCH and CaMSCH(NaCl) at 0.5 GPa. $p(CO_2)$ is the proportion of CO_2 in the solution, $\frac{CO_2}{CO_2+H_2O+NaCl,tot+aqSi}$. Solid line, $x_{NaCl,tot} = 0$; dotted line, $x_{NaCl,tot} = 0.05$; dashed line, $x_{NaCl,tot} = 0.1$. Addition of NaCl reduces the temperature of reactions with low $\frac{\partial T}{\partial X_{CO_2}}$ while other reactions are largely unaffected. Mineral abbreviations: di, diopside; dol, dolomite; tr, tremolite; ta, talc; cc, calcite; q, quartz. Quartz, fluid and calcite in excess.

in the temperature of calc-silicate equilibria, such as those shown in Fig. 7, could significantly increase the uncertainty on $X(CO_2)$ estimates made in this way.

10. Discussion

The DH–ASF model is thermodynamically valid over the range of P, T and composition space for which the assumptions that underlie the model are valid. This range includes pressures from 0.1 to 2 GPa and temperatures from 200 to 1000 °C. The use of water density in α parameter calculations (Section 8) restricts the model to solvents whose density varies in a similar way to that of water as a function of P and T. It is therefore strictly inapplicable to fluids with very low water content, although the success with which water-poor NaCl–H_2O (Section 9.1) and KCl–H_2O (Section 9.2) fluids are modelled suggests that such fluids may be modelled in some cases. The Debye–Hückel formulation is based on the assumption that the solvent forms a continuous medium with a constant dielectric constant. This assumption becomes invalid at low fluid densities or when water becomes ionized at very high pressures and temperatures ($P > 50$ GPa; Goncharov et al., 2005). The pressure limitation is unlikely to trouble most geochemists, but a minimum density of 0.5 is suggested for modelled fluids. A corollary of this restriction is that the model is not suitable for the low density phase in two phase fluids. Apart from these, the main restriction on use of the DH–ASF model is the limited availability of model parameters. It is therefore of interest to speculate on the degree to which calibrated parameters may be extrapolated and whether it is possible to estimate parameters for end-members without available data.

The extent to which any model may be extrapolated depends on the accuracy with which it represents the processes that occur in the modelled system. The more empirical a model, the less it should be extrapolated. The DH–ASF model is least empirical, and thus most successful, when the ideal mixing terms are correctly specified. If the ideal mixing is incorrectly specified then the activity coefficient is forced to compensate, and the extrapolative capacity of the parameters is weak, as in the case of the pressure-dependence of the NaCl–H_2O–SiO_2 dataset. Thus, the key to extrapolation of the model is knowledge of speciation, where speciation includes solvation, association and complex formation. Such data can be obtained from conductivity studies (e.g., Ho et al., 2000), via the use of Raman (e.g., Zotov and Keppler, 2000), infra-red or UV (e.g., Liu et al., 2001), or synchrotron spectroscopic techniques (e.g., Fulton et al., 1996). Care should be taken with extrapolation of parameters that relate to end-members present in small quantities, because these can be poorly constrained.

Systems that contain end-members for which calibration parameters are not available may be modelled, in some cases, by neglecting those that are unlikely to influence results by a significant amount. An example of this strategy that reduces the number of parameters required to $\frac{n_s}{2}(2n - n_s - 1)$, is discussed in Section 8.2.2. The activity coefficient of such end-members would still be different to one because of the contributions of the terms that account for the mixing of the more abundant end-members. Alternatively, relationships between known properties (e.g., ionic radius, heat capacity) of calibrated and uncalibrated end-members can be used to estimate values of the unknown calibration parameters. This approach is described in detail by Shock et al. (1992). However, there is currently no system that allows consistently reliable extrapolation of the calibration parameters to pressures and temperatures other than those of calibration.

11. Conclusions

The DH–ASF model is thermodynamically valid across a wide range of P, T and composition. It can be applied to the concentrated and mixed solvent supercritical solutions that occur in a wide range of geological environments, including coexisting melts and liquids. The distinctive features of this model are the explicit specification of speciation, the use of the mole fraction concentration scale, the unique permutation of previously extant Debye–Hückel and Van Laar activity coefficient model components, the dependency of the α parameter on the density of water, and the application of the limited Debye–Hückel equation.

The model has been tested and calibrated, for common end-members, by application to simple systems for which

well constrained laboratory data is available. The model can reproduce experimental results to within experimental error in most cases, and the values of calibrated parameters are consistent with expectations based on the physical background to the model development. Success of the model depends on correct identification of speciation in solution. Application of the model is hampered by a lack of experimental data for calibration. However, it may be possible to neglect parameters that make relatively insignificant contributions to the total excess energy of mixing. In this case, the approach to activity calculation presented here provides immediate opportunities for investigation of hitherto inaccessible geological systems. These include saline fluid:rock interactions, metasomatism of alkali metals and earths during metamorphism of calc-silicates, and ore-forming processes in highly saline (copper, lead, and zinc) and CO_2-rich (gold) environments.

Acknowledgments

K.E. acknowledges a postdoctoral fellowship from CSIRO Exploration and Mining, and honorary fellowships at the Universities of Melbourne and Monash. R.P. acknowledges support of ARC Discovery Grants DP0451770. Tim Holland, Neil Phillips, and Weihua Liu are thanked for helpful comments on previous versions of the manuscript, as are numerous reviewers, including Peter Tropper. We thank Eric Oelkers and William Casey for editorial assistance. John P. O'Connell is thanked for helpful discussions on the nature of the dielectric constant.

Associate Editor: Eric H. Oelkers

Appendix A

The use of the mole fraction concentration scale with literature values for the standard state potentials of aqueous end-members requires conversion of standard states from the hypothetical one molal, Henry's Law standard state ($a_i \to 1$ as $x_i \to 0$) to the pure hypothetical Raoult's Law standard state ($a_i \to 1$ as $x_i \to 1$). The superscripts m and x indicates properties related to the 1 molal standard state, and pure hypothetical standard states, respectively. The shift can be envisaged as occurring in two stages (Fig. A1). First, $\mu_i^{\ominus m}$ is augmented by the consequences of the compositional shift between the two standard states to produce the intermediate chemical potential μ_B:

$$\mu_B = \mu_i^{\ominus m} + RT \ln \frac{1}{x_i^{m=1}}. \tag{18}$$

Then, the contribution of the shift between Henry's Law and Raoult's Law is added:

$$\mu_i^{\ominus x} = \mu_B - RT \ln \gamma_{x=0}. \tag{19}$$

Note the negative sign of this contribution. The complete expression for the shift is

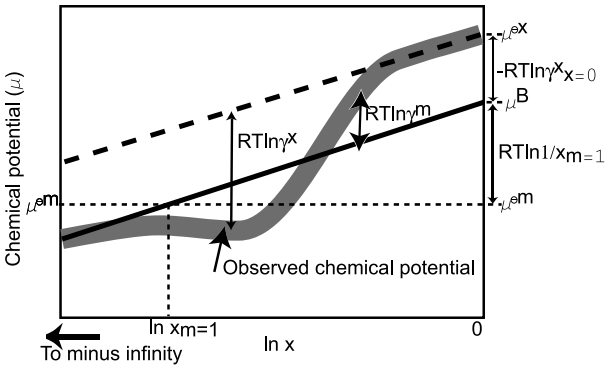

Fig. A1. Schematic illustration of the relationship between standard states. Thick line indicates measured chemical potential. Components of $\mu^{\ominus x}$ are shown. Solid line is the ideal potential ($\mu^{\ominus m} + RT \ln a_{id}$) of an ideal solution referenced to infinite dilution. Broken line is the chemical potential for an ideal solution referenced to a hypothetical ideal solution at $x = 1$.

$$\mu_i^{\ominus x} = \mu_i^{\ominus m} + RT \ln \frac{1}{x_{m=1}} - RT \ln \gamma_{x=0}. \tag{20}$$

Appendix B

Tables A2.A, A2.B, A2.C, A2.D, A2.E, A2.F give tabulated values of A_x and B_x for X(CO_2) values of 0, 0.1 and 0.2 for pressures between 0.3 and 1 GPa, and for temperatures between 300 and 800 °C.

Appendix C

C.1. Example of calculation of chemical potential for a H_2O–NaCl solution

The Gibbs Energy of a solution is given by Eq. (1) where the sum is over a set of independent end-members. Three end-members are required for the system H_2O–NaCl, where NaCl may dissociate. An appropriate set of end-members for the system is H_2O, associated NaCl ($NaCl^0$), and dissociated NaCl (NaCl±), which is used here. The chemical potential of each end-member in solution is given by Eqs. (4)–(10) and (15).

Water is present in solution as a species, as well as an end-member, so its ideal activity is its proportion. Commonly tabulated standard state data for this end-member uses a mole fraction of one, so it is not necessary to accommodate any change in standard state. Thus,

$$\begin{aligned}\mu_{H_2O} =& \mu_{H_2O}^{\ominus} + RT \ln p_{H_2O} + RT \ln \gamma_{H_2O,DH} + RT \ln \gamma_{H_2O,VL} \\ =& \mu_{H_2O}^{\ominus} + RT \ln p_{H_2O} + RT \frac{V_{H_2O} \kappa^3}{8\pi N_A} \sigma \\ &+ (1 - \phi_{H_2O}) \phi_{NaCl^0} W^*_{H_2ONaCl^0} \\ &+ (1 - \phi_{H_2O}) \phi_{NaCl\pm} W^*_{H_2ONaCl\pm} \\ &- \phi_{NaCl^0} \phi_{NaCl\pm} W^*_{NaCl^0NaCl\pm}\end{aligned}$$

Table A2.A
Values of A_x for $X(CO_2)$ equal to 0

P (GPa)/T (°C)	300	400	500	600	700	800
0.3	5.7195	6.8892	8.5999	10.714	13.183	15.842
0.4	5.3245	6.2908	7.6011	9.1303	10.853	12.703
0.5	5.0345	5.8731	6.9525	8.1665	9.4986	10.913
0.6	4.8075	5.5581	6.4871	7.5044	8.5982	9.7458
0.7	4.6221	5.3082	6.1315	7.0147	7.9489	8.9185
0.8	4.466	5.1027	5.8477	6.6339	7.4541	8.2973
0.9	4.3316	4.9292	5.6137	6.3266	7.0618	7.811
1	4.2138	4.7795	5.4161	6.0717	6.7411	7.4179

Table A2.B
Values of A_x for $X(CO_2)$ equal to 0.1

P (GPa)/T (°C)	300	400	500	600	700	800
0.3	7.566	9.08969	11.1809	13.642	16.3695	19.1577
0.4	6.91666	8.14347	9.72545	11.5046	13.4323	15.4208
0.5	9.03679	9.92066	10.9821	12.1424	13.3882	14.6846
0.6	6.08222	7.00512	8.10598	9.2809	10.5106	11.7661
0.7	5.78531	6.62131	7.59198	8.61006	9.66161	10.7271
0.8	5.54917	6.31981	7.19483	8.09961	9.02356	9.95274
0.9	5.35272	6.0723	6.87418	7.69359	8.52212	9.34945
1	5.18485	5.86329	6.60748	7.36042	8.11518	8.86387

Table A2.C
Values of A_x for $X(CO_2)$ equal to 0.2

P (GPa)/T (°C)	300	400	500	600	700	800
0.3	9.90883	11.8362	14.3142	17.0958	20.0365	22.9042
0.4	8.93335	10.4604	12.3294	14.3554	16.4701	18.5711
0.5	17.6208	18.0855	18.621	19.2446	19.9574	20.7335
0.6	7.72802	8.85161	10.1402	11.4792	12.8428	14.197
0.7	7.28515	8.2973	9.43189	10.5937	11.7645	12.9216
0.8	6.94679	7.87583	8.89733	9.93056	10.962	11.9756
0.9	6.67194	7.5366	8.47189	9.40816	10.3349	11.2405
1	6.44105	7.25426	8.12177	8.98257	9.82822	10.6499

Table A2.D
Values of B_x for $X(CO_2)$ equal to 0

P (GPa)/T (°C)	300	400	500	600	700	800
0.3	2.73158	2.83789	2.95474	3.06359	3.1578	3.23084
0.4	2.7049	2.80264	2.90535	2.99962	3.0826	3.1513
0.5	2.68462	2.77687	2.87079	2.95599	3.03124	3.09513
0.6	2.66826	2.75676	2.8447	2.92374	2.99348	3.05335
0.7	2.65449	2.74033	2.82399	2.89861	2.96429	3.02095
0.8	2.64258	2.72646	2.80695	2.8783	2.94089	2.99499
0.9	2.63204	2.71445	2.79254	2.86138	2.9216	2.97365
1	2.62257	2.70384	2.78007	2.84698	2.90533	2.95573

where

$$\phi_{H_2O} = \frac{p_{H_2O}\alpha_{H_2O}}{p_{H_2O}\alpha_{H_2O} + p_{NaCl^0}\alpha_{NaCl^0} + p_{NaCl\pm}\alpha_{NaCl\pm}},$$

$$W^*_{H_2ONaCl^0} = w_{H_2ONaCl^0}\frac{2\alpha_{H_2O}}{\alpha_{H_2O} + \alpha_{NaCl^0}},$$

$$W^*_{H_2ONaCl\pm} = w_{H_2ONaCl\pm}\frac{2\alpha_{H_2O}}{\alpha_{H_2O} + \alpha_{NaCl\pm}},$$

and

$$W^*_{NaCl^0NaCl\pm} = w_{NaCl^0NaCl\pm}\frac{2\alpha_{H_2O}}{\alpha_{NaCl^o} + \alpha_{NaCl\pm}},$$

Associated NaCl ($NaCl^0$) is also present in the solution as a species, so its ideal activity is, as for water, its proportion. The solute species has no charge, so the Debye–Hückel contribution to the chemical potential is zero, so long as the associated NaCl is considered to be solute rather than solvent. If salt is present in sufficient quantities to be considered as part of the solvent then the Debye–Hückel con-

Table A2.E
Values of B_x for $X(CO_2)$ equal to 0.1

P (GPa)/T (°C)	300	400	500	600	700	800
0.3	2.86559	2.97321	3.08486	3.18407	3.2652	3.32341
0.4	2.8294	2.92794	3.02697	3.11471	3.18882	3.2471
0.5	2.96058	3.02601	3.08892	3.14499	3.1936	3.23365
0.6	2.7791	2.8681	2.95378	3.02895	3.09347	3.14706
0.7	2.75987	2.84632	2.92827	2.99982	3.06128	3.11279
0.8	2.74414	2.82869	2.90782	2.9766	3.03564	3.08535
0.9	2.7307	2.81381	2.89078	2.95745	3.01458	3.06279
1	2.71892	2.80093	2.87623	2.94124	2.99687	3.04386

Table A2.F
Values of B_x for $X(CO_2)$ equal to 0.2

P (GPa)/T (°C)	300	400	500	600	700	800
0.3	3.01672	3.12385	3.22835	3.31655	3.38404	3.42746
0.4	2.97232	3.07052	3.16458	3.24469	3.30916	3.35652
0.5	3.31088	3.33958	3.36284	3.38151	3.39578	3.40507
0.6	2.91204	3.00068	3.08307	3.15336	3.21169	3.25815
0.7	2.8877	2.97411	3.0535	3.12111	3.17747	3.22301
0.8	2.8685	2.95318	3.03022	3.09567	3.15033	3.19486
0.9	2.85244	2.9358	3.01102	3.07479	3.12807	3.17168
1	2.83858	2.92093	2.99474	3.05721	3.10939	3.15221

tribution to the chemical potential would be as for water. Here it is assumed that standard state data for liquid NaCl (molten halite) is used, so it is not necessary to make any change to commonly available standard state data. The chemical potential of $NaCl^0$ is, therefore,

$$\begin{aligned}\mu_{NaCl^0} =& \mu^{\ominus}_{NaCl^0} + RT\ln p_{NaCl^0} + RT\ln\gamma_{NaCl^0,VL}\\ =& \mu^{\ominus}_{NaCl^0} + RT\ln p_{NaCl^0} + (1-\phi_{NaCl^0})\phi_{H_2O}W^*_{NaCl^0H_2O}\\ &+ (1-\phi_{NaCl^0})\phi_{NaCl\pm}W^*_{NaCl^0NaCl\pm}\\ &- \phi_{H_2O}\phi_{NaCl\pm}W^*_{H_2ONaCl\pm}\end{aligned}$$

where

$$\phi_{NaCl^0} = \frac{p_{NaCl^0}\alpha_{NaCl^0}}{p_{H_2O}\alpha_{H_2O} + p_{NaCl^0}\alpha_{NaCl^0} + p_{NaCl\pm}\alpha_{NaCl\pm}},$$

$$W^*_{NaCl^0H_2O} = w_{NaCl^0H_2O}\frac{2\alpha_{NaCl^0}}{\alpha_{H_2O}+\alpha_{NaCl^0}},$$

$$W^*_{NaCl^0NaCl\pm} = w_{NaCl^0NaCl\pm}\frac{2\alpha_{NaCl^0}}{\alpha_{NaCl^0}+\alpha_{NaCl\pm}},$$

and

$$W^*_{H_2ONaCl\pm} = w_{H_2ONaCl\pm}\frac{2\alpha_{\ NaCl^0}}{\alpha_{H_2O}+\alpha_{NaCl\pm}},$$

The end-member that represents dissociated NaCl (NaCl±) is not present in the solution as a species, so its ideal activity is more complicated than that of the two previous end-members. The ideal activity for mean ionic end-members is given by Eq. (5), and is a function of the proportions of the component ions Na^+ and Cl^-. In the absence of other salts the proportion of each of these ions is $\frac{p_{\ NaCl\pm}}{2}$, so the ideal activity is $\frac{p_{NaCl\pm}}{2}$. Standard state data for this end-member is traditionally given for the hypothetical 1 m solution referenced to infinite dilution. It is therefore necessary to adjust the standard state free energy to the hypothetical pure end-member, as described in Appendix A. The conversion is given by

$$\begin{aligned}\mu^{\ominus x}_{NaCl\pm} =& \mu^{\ominus m}_{NaCl\pm} + RT\ln\frac{1}{x_{m=1}} - RT\ln\gamma_{x=0}\\ =& \mu^{\ominus m}_{NaCl\pm} + RT\ln 57.556/2 - 2\frac{\alpha_{NaCl^0}}{\alpha_{NaCl^0}+\alpha_{H_2O}}\end{aligned} \quad (21)$$

It is not necessary to correct for the Debye–Hückel activity because this cancels against the adjustment necessary to give an activity of 1 at unit mole fraction. The chemical potential of NaCl± is then

$$\begin{aligned}\mu_{NaCl\pm} =& \mu^{\ominus}_{NaCl\pm} + RT\ln\frac{p_{NaCl\pm}}{2} + RT\ln\gamma_{NaCl\pm,DH} + RT\ln\gamma_{NaCl\pm,VL}\\ =& \mu^{\ominus}_{NaCl\pm} + RT\ln\frac{p_{NaCl\pm}}{2}\\ &- RT\frac{A_x\sqrt{I_x}}{1+\dot{a}B_x\sqrt{I_x}} + (1-\phi_{NaCl\pm})\phi_{H_2O}W^*_{NaCl\pm H_2O}\\ &+ (1-\phi_{NaCl\pm})\phi_{NaCl^0}W^*_{NaCl\pm NaCl^0} - \phi_{H_2O}\phi_{NaCl^0}W^*_{H_2ONaCl^0}\end{aligned}$$

where

$$\phi_{NaCl\pm} = \frac{p_{NaCl\pm}\alpha_{\ NaCl\pm}}{p_{H_2O}\alpha_{H_2O} + p_{\ NaCl^0}\alpha_{NaCl^0} + p_{NaCl\pm}\alpha_{NaCl\pm}},$$

$$W^*_{NaCl\pm H_2O} = w_{NaCl\pm H_2O}\frac{2\alpha_{\ NaCl\pm}}{\alpha_{H_2O}+\alpha_{NaCl\pm}},$$

$$W^*_{NaCl\pm NaCl^0} = w_{NaCl\pm NaCl^0}\frac{2\alpha_{NaCl\pm}}{\alpha_{NaCl^0}+\alpha_{NaCl\pm}},$$

and

$$W^*_{H_2ONaCl^0} = w_{H_2ONaCl^0}\frac{2\alpha_{NaCl\pm}}{\alpha_{H_2O}+\alpha_{NaCl^0}},$$

If the simplifications suggested in the text are made then all terms that do not involve H_2O vanish.

References

Abrams, D.S., Prausnitz, J.M., 1975. Statistical thermodynamics of liquid-mixtures—new expression for excess Gibbs energy of partly or completely miscible systems. *AiChE J.* **21**, 116–128.

Akinfiev, N., Zotov, A., 1999. Thermodynamic description of equilibria in mixed fluids (H_2O- non-polar gas) over a wide range of temperature (25–700 °C) and pressure (1-5000 bars). *Geochim. Cosmochim. Acta* **63**, 2025–2041.

Alt, J.C., Teagle, D.A.H., Brewer, T., Shanks, W.C., Halliday, A., 1998. Alteration and mineralization of an oceanic forearc and the ophiolite-ocean crust analogy. *J. Geophys. Res. Solid Earth* **103**, 12365–12380.

Anderko, A., Wang, P., Rafal, M., 2002. Electrolyte solutions: from thermodynamic and transport property models to the simulation of industrial processes. *Fluid Phase Equilib.*, 123–142.

Anderson, G.M., Burnham, C.W., 1965. The solubility of quartz in supercritical water. *Am. J. Sci* **263**, 494–511.

Anderson, G.M., Burnham, C.W., 1983. Feldspar solubility and the transport of aluminum under metamorphic conditions. *Am. J. Sci.*, 283–297.

Anderson, G.M., Crerar, D.A., 1993. *Thermodynamics in Geochemistry. The Equilibrium Model*. Oxford University Press, United Kingdom.

Anderson, G.M., Castet, S., Schott, J., Mesmer, R.E., 1991. The density model for estimation of thermodynamic parameters of reactions at high temperatures and pressures. *Geochim. Cosmochim. Acta* **55**, 1769–1779.

Aranovich, L.Y., Newton, R.C., 1996. H_2O activity in concentrated NaCl solutions at high pressures and temperatures measured by the brucite–periclase equilibrium. *Contrib. Mineral. Petrol.* **125**, 200–212.

Aranovich, L.V., Newton, R.C., 1997. H_2O activity in concentrated KCl and KCl–NaCl solutions at high temperatures and pressures measured using the brucite - periclase method. *Contrib. Mineral. Petrol.* **127**, 261–271.

Archer, D.G., Wang, P.M., 1990. The dielectric-constant of water and Debye–Hückel limiting law slopes. *J. Phys. Chem. Ref. Data* **19**, 371–411.

Ayers, J.C., Watson, E.B., 1991. Solubility of apatite, monazite, zircon, and rutile in supercritical aqueous fluids with implications for subduction zone geochemistry. *Philos. Trans. R. Soc. Lond. Ser. A Math. Phys. Eng. Sci.* **335**, 365–375.

Baker, J., Holland, T., Powell, R., 1991. Isograds in internally buffered systems without solid-solutions—principles and examples. *Contrib. Mineral. Petrol.* **106**, 170–182.

Blum, L., Hoye, J.S., 1977. Mean spherical model for asymmetric electrolytes. 2. Thermodynamic properties and pair correlation-function. *J. Phys. Chem.* **81**, 1311–1317.

Bockris, J.O., Reddy, A.K.N., 1998*Modern Electrochemistry*, Vol. 1. Plenum Press, New York.

Cabezas, H., O'Connell, J.P., 1993. Some uses and misuses of thermodynamic models for dilute liquid solutions. *Ind. Eng. Chem. Res.* **32**, 2892–2904.

Caciagli, N.C., Manning, C.E., 2003. The solubility of calcite in water at 6–16 kbar and 500–800 °C. *Contrib. Mineral. Petrol.* **146**, 275–285.

Cardoso, M.J.D., O'Connell, J.P., 1987. Activity coefficients in mixed solvent electrolyte solutions. *Fluid Phase Equilib.* **33**, 315–326.

Chen, C.-C., Song, Y., 2004. Generalized electrolyte-NRTL model for mixed-solvent electrolyte systems. *AiChE J.* **50**, 1928–1941.

Clegg, S.L., Pitzer, K.S., 1992. Thermodynamics of multicomponent, miscible, ionic-solutions—generalized equations for symmetrical electrolytes. *J. Phys. Chem* **96**, 3513–3520.

Clegg, S.L., Pitzer, K.S., Brimblecombe, P., 1992. Thermodynamics of multicomponent, miscible, ionic-solutions. 2. Mixtures including unsymmetrical electrolytes. *J. Phys. Chem.* **96**, 9470–9479.

Costagliola, P., Benvenuti, M., Maineri, C., Lattanzi, P., Ruggieri, G., 1999. Fluid circulation in the Apuane Alps core complex: evidence from extension veins in the Carrara marble. *Mineral. Mag.* **63**, 111–122.

Cox, S.F., 1995. Faulting processes at high fluid pressures: an example of fault valve behavior from the Wattle Gully Fault, Victoria, Australia. *J. Geophys. Res.* **100**, 12841–12859.

Crawford, M.L., Kraus, D.W., Hollister, L.S., 1979. Petrologic and fluid inclusion study of calc-silicate rocks, Prince-Rupert, British-Columbia. *Am. J. Sci.* **279**, 1135–1159.

Dale, J., Powell, R., White, R.W., Elmer, F.L., Holland, T.J.B., 2005. A thermodynamic model for Ca–Na clinoamphiboles in Na_2O–CaO–K_2O–FeO–Fe_2O_3–MgO–Al_2O_3–SiO_2–H_2O for petrological calculations. *J. Metamorph. Geol.* **23**, 771–791.

Davidson, N., 1962. *Statistical Mechanics*. McGraw-Hill, USA.

Davies, C.W., 1962. *Ion Association*. Butterworths, UK.

Debye, P., Hückel, E., 1923. Zur Theorie der Elektrolyte. I. Gefrierpunktserniedrigung und verwandte Erscheinungen. *Phys. Zeitschr* **24**, 185–206.

Duan, Z., Moller, N., Weare, J.H., 1995. Equation of state for the NaCl–H_2O–CO_2 system: prediction of phase equilibria and volumetric properties. *Geochim. Cosmochim. Acta* **59**, 2869–2882.

Ferry, J.M., 1994. Overview of the petrological record of fluid flow during regional metamorphism in northern New England. *Am. J. Sci.* **294**, 905–988.

Fulton, J.L., Pfund, D.M., Wallen, S.L., Newville, M., Stern, E.A., Ma, Y., 1996. Rubidium ion hydration in ambient and supercritical water. *J. Chem. Phys.* **105**, 2161–2166.

Gering, K.L., Lee, L.L., Landis, L.H., Savidge, J.L., 1989. A molecular approach to electrolyte-solutions—phase-behavior and activity- coefficients for mixed-salt and multisolvent systems. *Fluid Phase Equilib.* **48**, 111–139.

Gibert, F., Moine, B., Schott, J., Dandurand, J.-L., 1992. Modelling of the transport and deposition of tungsten in the scheelite-bearing calc-silicate gneisses of the Montagne Noire, France. *Contrib. Mineral. Petrol.* **112**, 371–384.

Goncharov, A.F., Goldman, N., Fried, L.E., Crowhurst, J.C., Kuo, I.F.W., Mundy, C.J., Zaug, J.M., 2005. Dynamic ionization of water under extreme conditions. *Phys. Rev. Lett.* **94**, 125508-1–125508-4.

Heinrich, H., Churakov, S.G., Gottschalk, M., 2004. Mineral-fluid equilibria in the system CaO–MgO–SiO_2–H_2O–CO_2–NaCl and the record of reactive fluid flow in contact metamorphic aureoles. *Contrib. Mineral. Petrol.* **148**, 131–149.

Helgeson, H.C., Kirkham, D.H., Flowers, G.C., 1981. Theoretical prediction of the thermodynamic behaviour of aqueous electrolytes at high pressures and temperatures: IV Calculation of activity coefficients, osmotic coefficients, and apparent molal and standard and relative partial molal properties to 600 °C and 5 kbar. *Am. J. Sci.* **281**, 1259–1516.

Ho, P.C., Bianchi, H., Palmer, D.A., Wood, R.H., 2000. Conductivity of dilute aqueous electrolyte solutions at high temperatures and pressures using a flow cell. *J. Soln. Chem.* **29**, 217–235.

Holland, T., Powell, R., 1996a. Thermodynamics of order-disorder in minerals 1. Symmetric formalism applied to minerals of fixed composition. *Am. Min.* **81**, 1413–1424.

Holland, T., Powell, R., 1996b. Thermodynamics of order-disorder in minerals 2. Symmetric formalism applied to solid solutions. *Am. Min.* **81**, 1425–1437.

Holland, T.J.B., Powell, R., 1998. An internally consistent thermodynamic data set for phases of petrological interest. *J. Met. Geol.* **16**, 309–343.

Holland, T., Powell, R., 2003. Activity–composition relations for phases in petrological calculations: an asymmetric multicomponent formulation. *Contrib. Mineral. Petrol.* **145**, 492–501.

Kennedy, G.C., Wasserburg, G.J., Heard, H.C., Newton, R.C., 1962. The upper three-phase region in the system SiO_2–H_2O. *Am. J. Sci.* **260**, 501–521.

Kirkwood, J.G., 1939. The dielectric polarization of polar liquids. *J. Phys. Chem.* **7**, 911–919.

Koster van Groos, A.F., 1991. Differential thermal analysis of the liquidus relations in the system NaCl–H_2O to 6 kbar. *Geochim. Cosmochim. Acta* **55**, 2811–2817.

Li, J., Polka, H.-M., Gmehling, J., 1994. A gE model for single and mixed solvent electrolye systems. 1. Model and results for strong electrolytes. *Fluid Phase Equilib.* **94**, 89–114.

Liu, W.H., McPhail, D.C., Brugger, J., 2001. An experimental study of copper(I)–chloride and copper(I)–acetate complexing in hydrothermal solutions between 50 degrees C and 250 degrees C and vapor-saturated pressure. *Geochim. Cosmochim. Acta* **65**, 2937–2948.

Lowenstern, J.B., 2001. Carbon dioxide in magmas and implications for hydrothermal systems. *Min. Dep.* **36**, 490–502.

Manning, C.E., 1994. The solubility of quartz in H_2O in the lower crust and upper mantle. *Geochim. Cosmochim. Acta* **58**, 4831–4839.

Newton, R.C., Manning, C.E., 2000. Quartz solubility in H_2O–NaCl and H_2O–CO_2 solutions at deep crust-upper mantle pressures and temperatures: 2–15 kbar and 500–900 °C. *Geochim. Cosmochim. Acta* **64**, 2993–3005.

Nordstrom, D.K., Munoz, J.L., 1994. *Geochemical Thermodynamics*. Blackwell Scientific Publications, United Kingdom.

O'Connell, J.P., 2003. Modeling the properties of mixed-solvent electrolyte solution, 19th European Seminar on Applied Thermodynamics, Santorini, Greece.

Oelkers, E.H., Helgeson, H.C., 1990. Triple-ion anions and polynuclear complexing in supercritical electrolyte-solutions. *Geochim. Cosmochim. Acta* **54**, 727–738.

Paillat, O., Elphick, S.C., Brown, W.L., 1992. The solubility of water in $NaAlSi_3O_8$ melts: a re-examination of Ab–H_2O phase relationships and critical behaviour ath high pressures. *Contrib. Mineral. Petrol* **112**, 490–500.

Pelton, A.D., Thompson, W.T., 1970. A structural model for magnesium chloride-containing melts. *Can. J. Chem.* **48**, 1585–1597.

Phillips, G.N., Powell, R., 1993. Link between gold provinces. *Econ. Geol.* **88**, 1084–1098.

Pitzer, K.S., 1973. Thermodynamics of electrolytes I. Theoretical basis and general equations. *J. Phys. Chem.* **77**, 268–277.

Pitzer, K.S., Simonson, J.M., 1986. Thermodynamics of multicomponent, miscible, ionic systems—theory and equations. *J. Phys. Chem.* **90**, 3005–3009.

Powell, R., 1977. Activity–composition relationships for crystalline solutions. In: Fraser, D.G. (Ed.), *Thermodynamics in Geology*. D. Reidel Publishing Company, pp. 57–66.

Powell, R., 1978. *Equilibrium Thermodynamics in Petrology*. Harper and Row, United Kingdom.

Powell, R., Holland, T.J.B., 1993. On the formulation of simple models for complex phases. *Am. Min.* **78**, 1174–1180.

Powell, R., Holland, T., Worley, B., 1998. Calculating phase diagrams involving solid solutions via non-linear equations, with examples using THERMOCALC. *J. Met. Geol.* **16**, 577–588.

Powell, R., Hergt, J., Woodhead, J., 2002. Improving isochron calculations with robust statistics and the bootstrap. *Chem. Geol.* **185**, 191–204.

Prausnitz, J., Lichtenthaler, R.N., de Azevedo, E.G., 1986. *Molecular Thermodynamics of Fluid-Phase Equilibria*. Prentice-Hall, U.S.A..

Renon, H., Prausnitz, J., 1968. Local compositions in thermodynamic excess functions for liquid mixtures. *AiChE J.* **14**, 135–150.

Rodil, E., Vera, J.H., 2003. The activity of ions: analysis of the theory and data for aqueous solutions of $MgBr_2$, $CaBr_2$ and $BaBr_2$ at 298.2 K. *Fluid Phase Equilib.* **205**, 115–132.

Shen, A.H., Keppler, H., 1997. Direct observation of complete miscibility in the albite–H_2O system. *Nature* **385**, 710–712.

Sherman, D.M., Collings, M.D., 2002. Ion association in concentrated NaCl brines from ambient to supercritical conditions: results from classical molecular dynamics simulations. *Geochem. Trans.* **3**, 102–107.

Shmulovich, K., Graham, C., Yardley, B., 2001. Quartz, albite and diopside solubilities in H_2O–NaCl and H_2O–CO_2 fluids at 0.5–0.9 GPa. *Contrib. Mineral. Petrol.* **141**, 95–108.

Shock, E.L., Oelkers, E.H., Johnson, J.W., Sverjensky, D.A., Helgeson, H.C., 1992. Calculation of the thermodynamic properties of aqueous species at high pressures and temperatures. *J. Chem. Soc. Faraday Trans.* **88**, 803–826.

Skippen, G., 1974. Experimental model for low-pressure metamorphism of siliceous dolomitic marble. *Am. J. Sci.* **274**, 487–509.

Skippen, G., Trommsdorff, V., 1986. The influence of NaCl and KCl on phase-relations in metamorphosed carbonate rocks. *Am. J. Sci.* **286**, 81–104.

Stalder, R., Foley, S.F., Brey, G.P., Horn, I., 1998. Mineral aqueous fluid partitioning of trace elements at 900–1200 degrees C and 3.0–5.7 GPa: new experimental data for garnet, clinopyroxene, and rutile, and implications for mantle metasomatism. *Geochim. Cosmochim. Acta* **62**, 1781–1801.

Stalder, R., Ulmer, P., Thompson, A.B., Gunther, D., 2000. Experimental approach to constrain second critical end points in fluid/silicate systems: near-solidus fluids and melts in the system albite–H_2O. *Am. Min.* **85**, 68–77.

Stokes, R.H., 1991. Thermodynamics of solutions. In: Pitzer, K.S. (Ed.), *Activity Coefficients in Electrolyte Solutions*. CRC Press, pp. 1–28.

Stokes, R.H., Robinson, R.A., 1948. Ionic hydration and activity in electrolyte solutions. *J. Am. Chem. Soc.* **70**, 1870–1878.

Thompson, J.B.J., 1982. Composition space: an algebraic and geometric approach. In: Ferry, J.M. (Ed.), *Characterisation of Metamorphism Through Mineral Equilibria*, *Reviews in Mineralogy*, Vol. 10. Mineralogical Society of America, pp. 1–31.

Trommsdorff, V., Skippen, G., Ulmer, P., 1985. Halite and sylvite as solid inclusions in high-grade metamorphic rocks. *Contrib. Mineral. Petrol.* **89**, 24–29.

Trommsdorff, V., Connolly, J.A.D., 1990. Constraints on phase-diagram topology for the system CaO–MgO–SiO_2–CO_2–H_2O. *Contrib. Mineral. Petrol.* **104**, 1–7.

Tropper, P., Manning, C.E., 2004. Paragonite stability at 700 °C in the presence of H_2ONaCl fluids: constraints on H_2O activity and implications for high pressure metamorphism. *Contrib. Mineral. Petrol.* **147**, 740–749.

Truesdell, A.H., Jones, B.F., 1974. WATEQ, a computer program for calculating chemical equilibria of natural waters. *J. Res. US Geol. Surv.* **2**, 233–274.

Van Laar, J.J., 1906. *Sechs Vortrage uber das Thermodynamische Potential und seine Anwendungen auf chemische und physikalische Gleichgewichtsprobleme eingeleitet durch zwei Vortrge ber nichtverdnnte Lsungen und ber den Osmotischen Druck*. Friedrich Vieweg und sohn, Brunswick.

Walther, J.V., 1992. Ionic association in H_2O and CO_2 fluids. *J. Met. Geol.* **10**, 789–797.

Wang, P., Anderko, A., Young, E.D., 2002. A speciation-based model for mixed-solvent electrolyte systems. *Fluid Phase Equilib.* **203**, 141–176.

White, R.W., Powell, R., Holland, T.J.B., 2001. Calculation of partial melting equilibria in the system Na_2O–CaO–K_2O–FeO–MgO–Al_2O_3–SiO_2–H_2O (NCKFMASH). *J. Met. Geol.* **19**, 139–153.

Wilczek-Vera, G., Rodil, E., Vera, J.H., 2004. On the activity of ions and the junction potential: revised values for all data. *AiChE J.* **50**, 445–462.

Xie, Z.X., Walther, J.V., 1993. Quartz solubilities in NaCl Solutions with and without wollastonite at elevated-temperatures and pressures. *Geochim. Cosmochim. Acta* **57**, 1947–1955.

Zotov, N., Keppler, H., 2000. In situ Raman spectra of dissolved silica species in aqueous fluids to 900 °C and 14 kbar. *Am. Min.* **85**, 600–604.

Zotov, N., Keppler, H., 2002. Silica speciation in aqueous fluids at high pressures and high temperatures. *Chem. Geol.* **184**, 71–82.